ACS OMEGA

Open Access

This article is licensed under CC-BY-NC-ND 4.0

http://pubs.acs.org/journal/acsodf

Article

Chitosan-Starch Biocomposite for Enhanced Curcumin Delivery: Kinetic Modeling of pH and Ionic Strength Responsive Release and Evaluation of Biological Efficacy

Lumini Abeywickrama, Supuni Wijayawardana, Charitha Thambiliyagodage,* and Madara Jayanetti

Cite This: *ACS Omega* 2026, 11, 41667−41688

Read Online

ACCESS | Metrics & More | Article Recommendations | Supporting Information

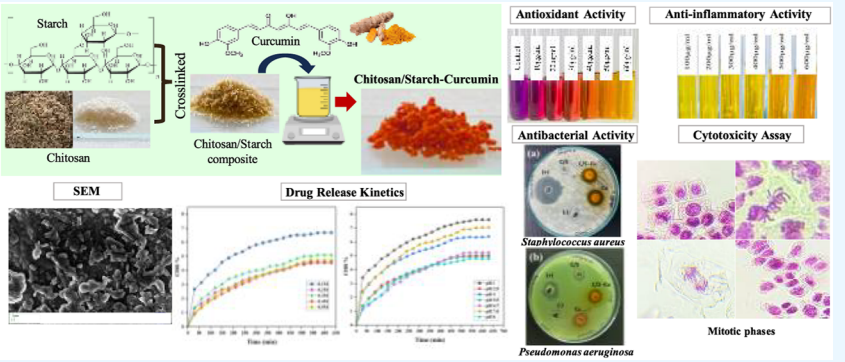

ABSTRACT: A drug delivery system composed of chitosan and starch was used to deliver curcumin effectively by enhancing its pharmacokinetic properties. The sustained release of the synthesized delivery system was evaluated using a kinetic modeling approach along with its biological efficacy. The SEM analysis confirmed the coupling of starch and chitosan and loading of curcumin into the matrix during synthesis. Crystallographic orientation of the delivery system was confirmed by XRD, and the FT-IR data confirmed the successful loading of curcumin. TG analysis indicated that the increment in decomposition temperature of the composite is due to the incorporation of curcumin into the composite. BET analysis revealed the reduction in the BET surface area and pore volume in the synthesized composite, confirming successful loading. The IC_{50} values of the curcumin and composite for the DPPH assay were 17.81 μg/mL and 38.77 μg/mL, respectively. Composite material has shown enhanced antibacterial activity against *Staphylococcus aureus* and *Pseudomonas aeruginosa* at 20 mg/mL, with inhibition zones of 15.56 ± 0.29 and 10.11 ± 0.44 mm, respectively. *Allium cepa* cytotoxicity assay confirmed that all the synthesized materials promote mitosis at 2.5 mg/mL concentration. The pH and ionic strength responsive release of curcumin was studied by fitting the release data into six kinetic models, including Korsemeyer−Peppas (KP) and Peppas−Sahlin (PS), which has not been reported earlier for the synthesized system. The KP and PS models were selected to interpret the release mechanism based on R^2. A combination of Fickian diffusion, relaxation and swelling dominates the curcumin release. According to the KP model, quasi-Fickian diffusion is responsible for the release in acidic and alkaline pH, whereas non-Fickian diffusion occurs at pH 6.7. At higher [NaCl], relaxation is responsible for the release ($n > 0.43$, $k_D = 0$), while a combination of diffusion and relaxation governs the release at lower [NaCl]. These behaviors are related to the chemical composition of chitosan and the release media, where the electrostatic repulsion, protonation and charge screening contribute to curcumin release.

1. INTRODUCTION

Turmeric (*Curcuma longa* L.) is a perennial herbaceous plant belonging to the Zingiberaceae family. Curcumin, a hydrophobic bioactive polyphenolic compound, is the most studied curcuminoid of the plant rhizome, which has been used as a remedy for disease conditions from ancient times.[1] The chemical structure of curcumin consists of two ortho-methoxy phenolic groups that are connected symmetrically to a β-diketone moiety.[2] Curcumin is well-known for its antioxidant,[3] anti-inflammatory,[4] antibacterial,[5] anticancer,[6] neuroprotective[7] and hepatoprotective[8] activities. Interestingly, the anticancer activity of curcumin is discussed widely and related to many cancer types, including colon,[9] breast,[10] prostate,[11] esophagus,[12] lung cancers[13] and multiple myeloma.[14] However, low bioavailability is attributed to poor water solubility,

Received: February 1, 2026
Revised: June 19, 2026
Accepted: June 29, 2026
Published: July 2, 2026



© 2026 The Authors. Published by American Chemical Society

Downloaded from pubs.acs.org/acsodf/article-pdf/11/28/41667/6540397/acsomega.6c01210.pdf by guest on 15 August 2026

rapid metabolism and elimination[15] and limited gut absorption[2] limits the therapeutic use of curcumin. The half-life of curcumin in pH 7.4 phosphate buffer was reported to be only 10 min2 and the plasma concentration is limited even after consuming higher concentrations. Therefore, strategies like polymeric[16] nanoparticle[17] delivery systems, nanoemulsions[18] and coadministration of curcumin with other bioactive compounds[19] have been employed to enhance the solubility and bioavailability of curcumin.

Chitosan is a linear biopolymer characterized by partial deacetylation, composed of randomly dispersed β-(1−4)-linked D-glucosamine (deacetylated unit) and *N*-acetyl-D-glucosamine units connected by glycosidic linkages.[20] Owing to its superior biomedical properties including bio/hemo compatibility, biodegradability, mucoadhesivity, anticancer, and antimicrobial activities, chitosan has been commonly employed in drug delivery systems.[21] Aslzad et al. has developed an enzyme-responsive carrier for doxorubicin (DOX) using chitosan/gelatin nanogel with gold nanoparticles.[22] In a study conducted by Jalaladdiny et al. chemotherapeutic agent, DOX, was coencapsulated with curcumin using a metal−organic framework coated with folic acid and chitosan.[23] Furthermore, chitosan was used as a component of the delivery system composed of poly(vinylpyrrolidone)/γ-Alumina nanocomposite for the delivery of quercetin by Nematollahi et al.[24] Therefore, chitosan facilitates the protection of the unstable bioactive substance and ensures the targeted and regulated delivery of pharmaceuticals to specific locations, consequently improving the therapeutic efficacy and reducing the frequency and dosage of administration.

Starch is a polysaccharide of amylopectin, which consists of 1−4 and 1−6 α-D-glucopyranose units and amylose, which is a linear polymer with 1−4 α-D-glucopyranose units.[25] As a naturally abundant, biodegradable polysaccharide, it has been gaining attention in the scientific community to be used in pharmaceutical applications because of its biocompatible, nontoxic and nonimmunogenic nature.[26] Alipournazari et al.[27] employed a pH-sensitive starch/PVA and graphitic carbon nitride hydrogel, and Gholamali et al.[28] used a delivery system with oxidized starch/poly(vinyl alcohol)/CuO bionanocomposite hydrogel for the delivery of DOX. Not only synthetic drugs, but a starch-based Pickering emulsion was developed for the delivery of resveratrol to the skin with sustained release properties by Bi et al.[29] Moreover, as demonstrated by Rajabpour et al.[30] and Parvaneh et al.[31] a curcumin-loaded hydrogel consisting of starch/agarose/ZnO can effectively target breast cancer cells, while carboxymethyl cellulose/starch/reduced graphene oxide composite can act as a pH-sensitive nanocarrier for curcumin. Starch is most commonly used as a stabilizer, filler or binder in drug delivery applications, and it facilitates controlled and sustained release of therapeutic agents.[32] In this work, starch was used as a secondary biopolymer with chitosan to enhance the stability of the chitosan polymeric network by acting as a filler, facilitating a pH-independent swelling, resulting in a smoother release. Further, starch can enhance the encapsulation efficiency of hydrophobic curcumin with chitosan, *via* hydrogen bondings between carbonyl (C═O) and phenolic (−OH) groups of curcumin.

As discussed above, chitosan and starch-based delivery systems have been used for the delivery of pharmacologically active natural substances, including curcumin,[33] resveratrol,[34] quercetin,[35] eugenol[36] and gallic acid[37] and many other synthetic therapeutic agents. Additionally, several studies have reported the use of chitosan/starch composite along with some other components. Sarmah et al.[38] and Nguyen et al.[39] have developed a self-cross-linked starch/chitosan hydrogel and a chitosan/starch nanocomposite for the ampicillin delivery, respectively. Furthermore, chitosan/starch-based delivery systems have been used to effectively deliver curcumin and curcumin analogues in the literature. A delivery system consisting of chitosan/starch/MoS_2 nanocomposite has been reported by Omrani et al.[40] and chitosan−starch nanocomposite particles used by Subramanian et al.,[41] to deliver curcumin targeting breast cancer treatment. Jo et al.[42] used a Pickering emulsion system consisting of starch crystals and chitosan to overcome the issues related to stability issues of curcumin in the GI tract. Consequently, in the present work, a biopolymeric delivery system consisting of chitosan/starch was synthesized using PVA as a stabilizer and glutaraldehyde as a cross-linker.

Curcumin was postcoated onto the chitosan/starch polymeric system to synthesize the curcumin-loaded chitosan/starch composite. The *in vitro* drug release kinetics of the delivery system were evaluated using six kinetic models under varying media compositions. The antibacterial activity of the synthesized samples was evaluated using *Staphylococcus aureus*, *Escherichia coli*, *Klebsiella pneumoniae* and *Pseudomonas aeruginosa* bacterial strains. Previously reported chitosan-based curcumin delivery systems typically have focused on the synthesis and evaluated the biological efficacy of the drug delivery system. However, to our knowledge, a detailed release kinetics analysis over a varied pH range and ionic strength conditions has not been reported in the literature for the delivery of curcumin using a chitosan/starch biopolymeric delivery system. In addition, the antibacterial activity of the curcumin-loaded composite has been studied thoroughly using Gram negative and Gram-positive bacterial strains in the current study. Therefore, the present study provides valuable information about the pH and ionic strength responsive release mechanism of curcumin from chitosan/starch composite and the biological effectiveness, specifically focusing on antibacterial activity evaluation, of the curcumin-loaded composite, addressing the key gaps in the current research. This integrated approach provides more sophisticated data on the release profile of the curcumin that can be used in optimization of the therapeutic potential in medical applications.

2. METHODOLOGY

Detailed methodology is described in the Supporting Information (Section 1: Materials and methodology).

2.1. Synthesis of Chitosan

Chitosan was synthesized using shrimp shells according to the methodology described by Mendis et al.[43] (Supporting Information Section 1.1).

2.2. Extraction of Curcumin

Local turmeric rhizomes (*Curcuma longa* L.) were used to prepare the ethanolic extract of curcumin, and samples were stored in -4 °C until further use[44] (Supporting Information Section 1.2).

2.3. Preparation of Chitosan/Starch Composite

Chitosan and gelatinized starch were mixed 1:1, combined with PVA solution, and stirred at 50 °C to form a gel. Glycerol

Downloaded from pubs.acs.org/acsodf/article-pdf/11/28/41667/6540397/acsomega.6c01210.pdf by guest on 15 August 2026

https://doi.org/10.1021/acsomega.6c01210
ACS Omega 2026, 11, 41667−41688

and glutaraldehyde were added, then the product was washed to neutral pH and dried at 45 °C for 24 h.[45] (Supporting Information Section 1.3).

2.4. Loading of Curcumin onto the Composite

Chitosan-starch composite (1 g) was added to the curcumin extract in ethanol and stirred at 300 rpm for 3 days at room temperature until it was fully evaporated. It was kept in the oven at 40 °C to obtain a dried powder (Supporting Information Section 1.4).

2.5. Material Characterization

XRD, SEM, FT-IR, BET, and TGA were conducted for the synthesized materials to study their crystallographic orientation, surface morphology, functional group variation, surface and pore size analysis and thermal stability, respectively (Supporting Information Section 1.5).

2.6. DPPH Antioxidant Assay

A DPPH (2,2-diphenyl-1-picrylhydrazyl) assay was used to determine the antioxidant potential of curcumin and the composite according to the method reported by Wijayawardana et al.,[44] (Supporting Information Section 1.6).

$$\text{scavenging effect (\%)} = \frac{A_{bc} - A_{bs}}{A_{bc}} \times 100\% \quad (1)$$

2.7. Anti-Inflammatory Assay

The *in vitro* anti-inflammatory activity of the curcumin extract and drug composites was determined using an egg albumin denaturation assay[44] (Supporting Information Section 1.7).

$$\text{\%activity remaining} = \frac{\text{absorbance of the test sample}}{\text{absorbance of the test control}} \times 100\% \quad (2)$$

2.8. Antibacterial Activity Determination—Agar Well Diffusion

The agar well diffusion method was conducted to determine the antibacterial activity of the synthesized samples (curcumin, chitosan, starch, chitosan-starch, and curcumin composite) using *E. coli*, *P. aeruginosa*, *K. pneumoniae*, and *S. aureus* as the test organisms[46] (Supporting Information Section 1.8).

2.9. *Allium cepa* Cytotoxicity Assay

A. cepa cytotoxicity assay was conducted to test the general toxicity and cytotoxicity of the synthesized samples, with slight modifications to the method reported by[47,48] (Supporting Information Section 1.9).

Mitotic index was calculated using the following equation.

$$\text{Mitotic index} = (\text{number of dividing meristematic cells} / 1000 \text{ total meristematic cells}) \times 100 \quad (3)$$

2.10. Loading Efficiency of Curcumin

The absorbance of free curcumin, resulting from the sample dissolution, was measured at 423 nm with proper dilutions. The Curcumin content was determined using a regression equation derived from the calibration curve of Curcumin. The following formula was used to determine the percentage of curcumin loading efficiency onto chitosan-starch composite (Supporting Information Section 1.10).

$$\text{loading efficiency\%} = \frac{\text{amount of the drug loaded (mg)}}{\text{total weight of the drug + system (mg)}} \times 100\% \quad (4)$$

2.10.1. Storage Stability of the Curcumin in the Composite. The stability of the synthesized compound was tested by comparing the loading efficiency of the freshly synthesized composite and the same composite after 6 months of storage at room temperature. The concentration of free curcumin in the supernatant was measured to determine the amount of curcumin that had either been released or leached from the composite over time (Supporting Information Section 1.10.1).

2.11. *In Vitro* Drug Release Kinetics of Curcumin

In vitro drug release of the synthesized drug delivery systems was assessed in different pH values, pH 1, pH 2.5, pH 4, pH 5.5, pH 7, pH 7.4, and pH 8, and ionic strengths in the range of 0.1−0.5 M, separately. Typically, the composite of interest (5 mg) was added into a cuvette with the respective release media (pH solution or NaCl solution) and the release data were collected every 15 min for 10 h.

The data from *in vitro* drug release studies were evaluated by various mathematical models, namely, Zero-order, First-order, Higuchi, Hixson−Crowell, Korsemeyer−Peppas models, and Peppas-Sahlin. The Cumulative drug release (CDR)% for every media composition was calculated using the following equation[49] (Supporting Information Section 1.11).

$$\%\text{CDR} = \frac{\text{amount released at time } (t)}{\text{total amount of drug loaded into DDS}} \times 100\% \quad (5)$$

2.12. Statistical Analysis

Triplicated data from DPPH antioxidant assay, egg albumin denaturation assay, antibacterial activity, and drug release analysis were statistically analyzed using SPSS Statistics (Version 27, SPSS Inc., Chicago, Illinois, USA), and results were expressed as mean ± standard error (SE). The confidence level of 95% was set as the Statistical significance. One-way analysis of variance (ANOVA) was used to determine the differences among the treatment means (Supporting Information Section 1.12).

3. RESULTS AND DISCUSSION

3.1. FT-IR Analysis

FT-IR spectra were collected to identify the chemical nature of the synthesized materials and to confirm the coating of curcumin on the biopolymer composite (Figure 1). The FT-IR spectrum of chitosan shows peaks in the range of 1010−1090 cm^{-1} attributed to the C−O stretching of the polysaccharide chain, and the peak at 1154 cm^{-1} is ascribed to the C−O−C vibration of the glycosidic linkage in the polymer chain. The peaks at 1376 cm^{-1} and 1422 cm^{-1} represent the CH_2 bending and CH_3 symmetrical deformations, respectively. The peak at 1556 cm^{-1} corresponds to the N−H bending of the amide II structure, and the peak at 1620 cm^{-1} represents the N−H bending of the primary amine (NH_2) in the chitosan structure. The peak at 1655 cm^{-1} is ascribed to the C═O stretching of amide I, suggesting the presence of residual N-acetyl groups. The peaks in the range of 2872−2961 cm^{-1} are attributed to the C−H symmetric and asymmetric stretching, respectively,

Downloaded from pubs.acs.org/acsodf/article-pdf/11/28/41667/6540397/acsomega.6c01210.pdf by guest on 15 August 2026

https://doi.org/10.1021/acsomega.6c01210
ACS Omega 2026, 11, 41667−41688

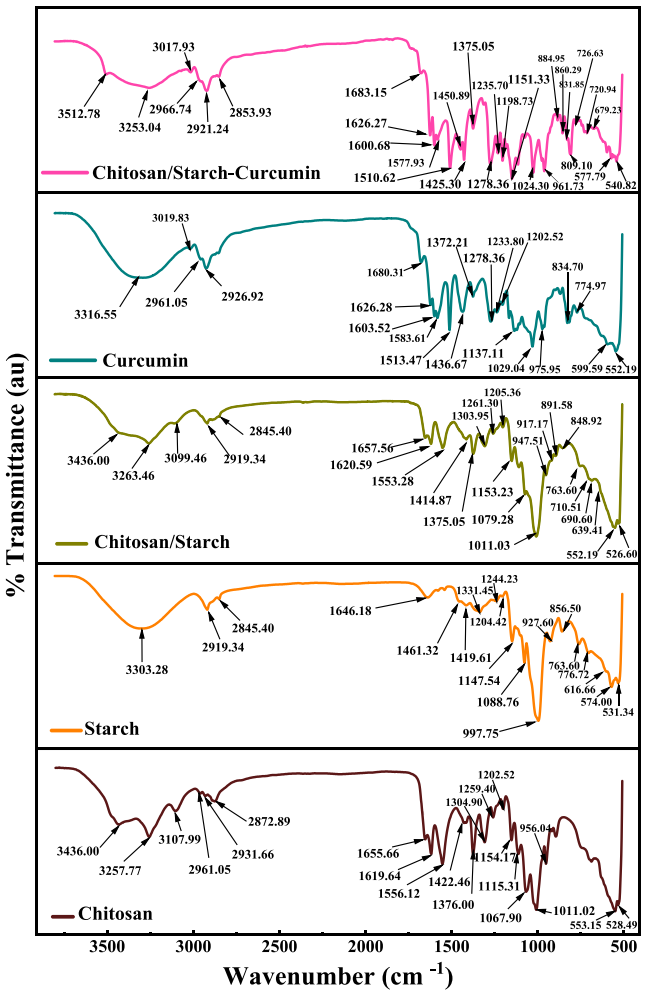

Figure 1. FT-IR Spectra of the synthesized chitosan, starch, extracted curcumin, and their composites.

which appear due to the presence of CH_2 bonds in the ring structures of the polysaccharide chain. The peak at 3258 cm^{-1} corresponds to the O−H stretching, and the broad peak at 3436 cm^{-1} is ascribed to the N−H stretching of the primary amine. The FT-IR spectrum of starch shows the characteristic peaks confirming the structure. The peak at 997.75 cm^{-1} corresponds to the C−O−C ring vibrations, and the peak at 1088.76 cm^{-1} represents the C−O stretching. The peak at 1147.54 cm^{-1} is attributed to the C−O−C asymmetric stretching, and the peaks at 1419.61 and 1461.32 cm^{-1} are ascribed to the CH_2 scissoring and deformations. The peak at 1646.18 cm^{-1} corresponds to the C−O bending, and the peak at 2919.34 cm^{-1} represents the C−H stretching of CH_2 groups. The peak at 3303.28 cm^{-1} reveals the presence of O−H groups. The FT-IR spectrum of chitosan/starch composite shows similar peaks found in the individual components, but with slight changes in the peak positions due to their coupling. In the chitosan/starch composite, the O−H stretching band shifted from 3258 cm^{-1} (chitosan) and 3303 cm^{-1} (starch) to a single intermediate broad band at 3280 cm^{-1}, indicating intermolecular hydrogen bond formation between the hydroxyl groups of the two polymers. The FT-IR spectrum confirms the structure of curcumin. The peaks in the range of 1137−1168 cm^{-1} correspond to the C−O stretching in ether linkages, and the peak at 1278.36 cm^{-1} is attributed to the C−O stretching of the phenolic groups. The peak at 1372.21 cm^{-1} is ascribed to the CH_3 bending, and the peak at 1436.67 cm^{-1} corresponds to the C−H bending and aromatic ring stretching. The prominent peak at 1513.47 cm^{-1} represents the stretching carbonyl bond vibrations, and the peak at 1603.52 cm^{-1} represents the C═C aromatic stretching. The peak at 1626.28 cm^{-1} is attributed to the C═O stretching, and the peaks at 2926.92 and the shoulder peak at 2961.05 cm^{-1} are ascribed to the CH_2 stretching vibrations. The broad peak at 3316.55 cm^{-1} corresponds to the O−H stretching vibration. Following curcumin loading, the N−H bending of chitosan (amide II) shifted from 1556 cm^{-1} to 1540 cm^{-1} (Δ = 16 cm^{-1} shift to lower wavenumber), suggesting hydrogen bonding between the amine groups of chitosan and the carbonyl or hydroxyl groups of curcumin. Additionally, the C═O stretching (amide I) shifted from 1655 cm^{-1} in pure chitosan to 1626 cm^{-1} in the curcumin-loaded composite (Δ = 29 cm^{-1}), further confirming hydrogen bond formation involving the carbonyl group. New peaks characteristic of curcumin appeared in the loaded composite at 1278 cm^{-1} (C−O phenolic stretching) and 1600 cm^{-1} (C═C aromatic stretching), confirming successful curcumin incorporation. The reduced intensity of the free N−H band at 1566 cm^{-1} is consistent with glutaraldehyde-mediated cross-linking of chitosan. Furthermore, the modest peak shifts (16−29 cm^{-1}) and lack of new major peaks indicate that curcumin interacts with the matrix through noncovalent interactions (primarily hydrogen bonding) rather than covalent conjugation. The coating is facilitated by the H- bond formation, suggesting that the curcumin has interacted with the chitosan/starch matrix upon loading. The peaks corresponding to curcumin being present in addition to those of chitosan and starch in chitosan/starch/curcumin composite suggest that chitosan/starch polymer composite has been successfully coated with curcumin.

3.2. BET Analysis

Brunauer−Emmett−Teller (BET) surface area analysis was performed to study the surface area and pore size distribution of the unloaded samples (chitosan, starch, and chitosan/starch). Figure 2(a,b) represent the adsorption−desorption isotherms and the pore size distribution graphs, respectively, and Table 1 summarizes the specific surface area, average pore diameters, and pore volume data of the synthesized materials. Chitosan, starch, and chitosan/starch composite exhibit a Type IV isotherm with H3 hysteresis loop as defined by IUPAC. The gradual increase in nitrogen uptake at low relative pressure corresponding to the monolayer adsorption on mesoporous material has reached a plateau at higher relative pressure (P/P_0 = 1) following capillary condensation and multilayer adsorption on the surface of the materials. The difference between the adsorption and desorption branches of the isotherm suggests the presence of pores with complex shapes. The surface area and the total pore volumes of the synthesized materials are comparatively lower, demonstrating a limited abundance in accessible micro and mesopores. Pore diameter data, which range between 2 and 4 nm, suggest that the porous system of all the synthesized materials consists of mesopores. Furthermore, the pore distribution of the synthesized material is nonuniform with multiple peaks, as shown in Figure 2 (b). Chitosan has the most developed porous structure among the tested samples, with the highest BET surface area (4.43 m^2/g) and pore volume (0.008 cm^3/g), in contrast to the smaller mesopore structure of starch. The surface area and the total

Downloaded from pubs.acs.org/acsodf/article-pdf/11/28/41667/6540397/acsomega.6c01210.pdf by guest on 15 August 2026

https://doi.org/10.1021/acsomega.6c01210
ACS Omega 2026, 11, 41667−41688

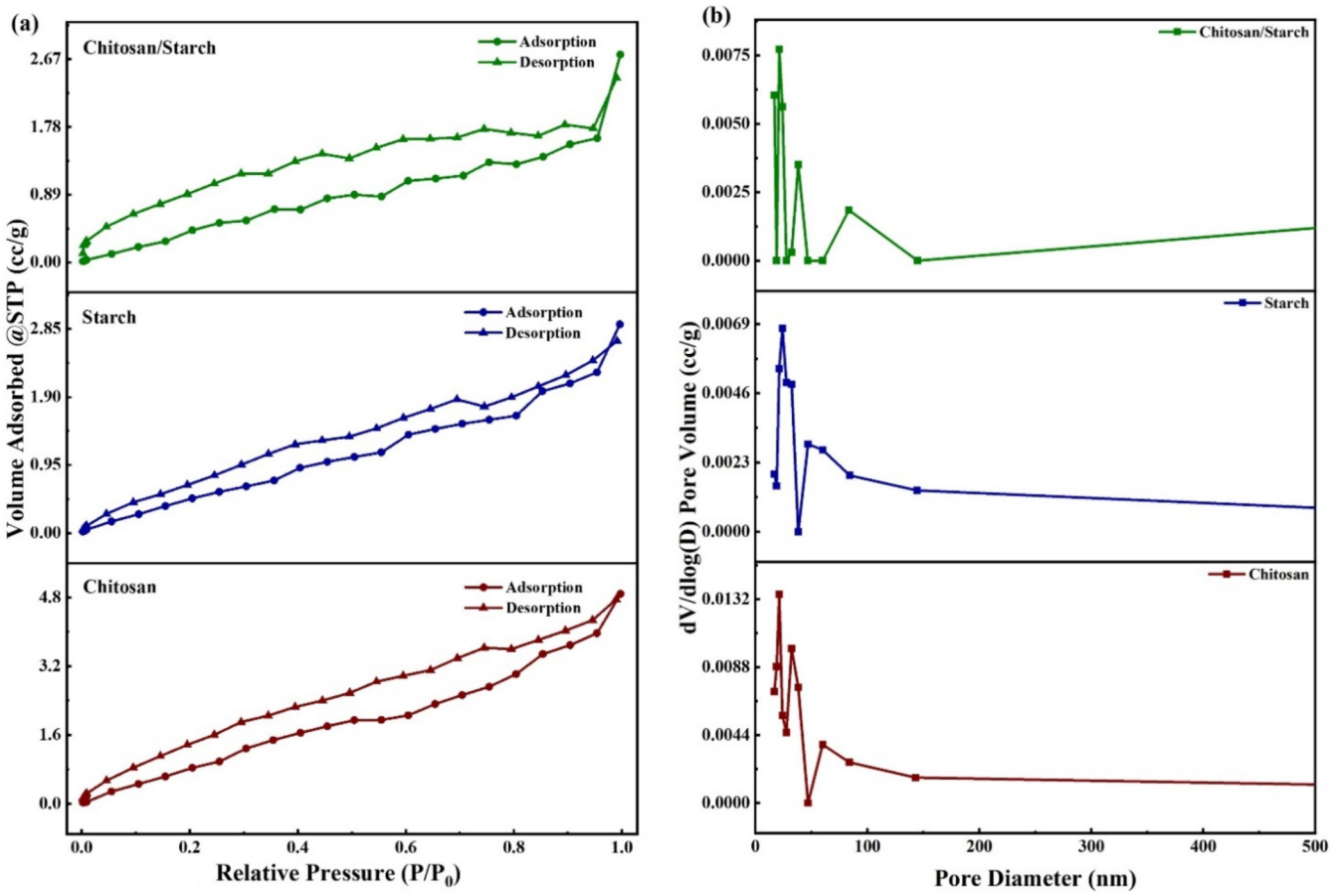

Figure 2. (a) Adsorption and desorption isotherms and (b) BJH pore size distribution curves of the synthesized materials.

Table 1. BET Surface Area, Pore Size, and Pore Volume Distribution of Synthesized Samples

sample	BET surface area (m^2/g)	average pore size (nm)	pore volume (cm^3/g)
chitosan	4.434	3.409	0.008
starch	3.640	2.477	0.005
chitosan/starch	2.390	3.535	0.004

pore volume of the chitosan/starch composite have been reduced to 2.40 m^2/g and 0.0004 cm^3/g, suggesting the successful incorporation of starch in the porous network and on the surface of chitosan. The increase in the average pore size (3.54 nm), compared to chitosan and starch, indicates the formation of larger mesopores during the composite material syntheses. While BET analysis of the curcumin-loaded composite was excluded due to the thermal sensitivity of curcumin, SEM imaging provides complementary evidence for pore filling. The oval-shaped pores visible in the unloaded composite are absent after curcumin loading (Figure S2(b,c)), indicating that the pores have been occupied by the drug during the loading process. The gas sorption data are supported by SEM surface morphology of pore filling, indicating that the reason for the reduction in the surface area and pore volume is drug loading within the pores rather than structural collapse.

The materials synthesized were characterized by XRD to study their crystallography (Figure S1 and Table S2), SEM to image the surface morphology (Figure S2), and TGA to evaluate the thermal stability (Figure S3), which are described in detailed in the Supporting Information Sections 2.1, 2.2, and 2.3, respectively.

3.3. Antioxidant Assay

The antioxidant activity of the curcumin extract and chitosan/starch-curcumin composites is illustrated in Figure 3. These results have shown that the IC_{50} of Curcumin extract was 17.81 μg/mL, suggesting that curcumin has a higher antioxidant activity. The linear regression model results in higher R^2 values (R^2 = 0.99) for both the curcumin extract and the chitosan/starch composite, as shown in Figure 3. The lack of plateau effects in the radical scavenging activity (RSA%) profiles indicates that saturation was not attained, as all values stayed within the linear response range.[50] Curcumin's ability to scavenge free radicals (DPPH) increased with higher concentrations. The RSA% of the curcumin extract was tested in the concentration range of 5−30 μg/mL in the current study, where the RSA% ranged between 15.71 ± 1.10−81.73 ± 0.52% in a dose-dependent manner. The RSA% values were no longer within the linear range of the dose-dependent relationship for the concentrations above 30 μg/mL, suggesting the potential saturation effect of DPPH radicals. Lower IC_{50} values ranging from 1.08 μg/mL−16.55 μg/mL were obtained in a work carried out by Tanvir et al.[51] using different turmeric varieties, similar to the current study. A study conducted by Ciochina et al.[52] have reported that curcumin and Trolox have extremely similar scavenging properties, according to the DPPH radical scavenging activity,

Downloaded from pubs.acs.org/acsodf/article-pdf/11/28/41667/6540397/acsomega.6c01210.pdf by guest on 15 August 2026

https://doi.org/10.1021/acsomega.6c01210
ACS Omega 2026, 11, 41667−41688

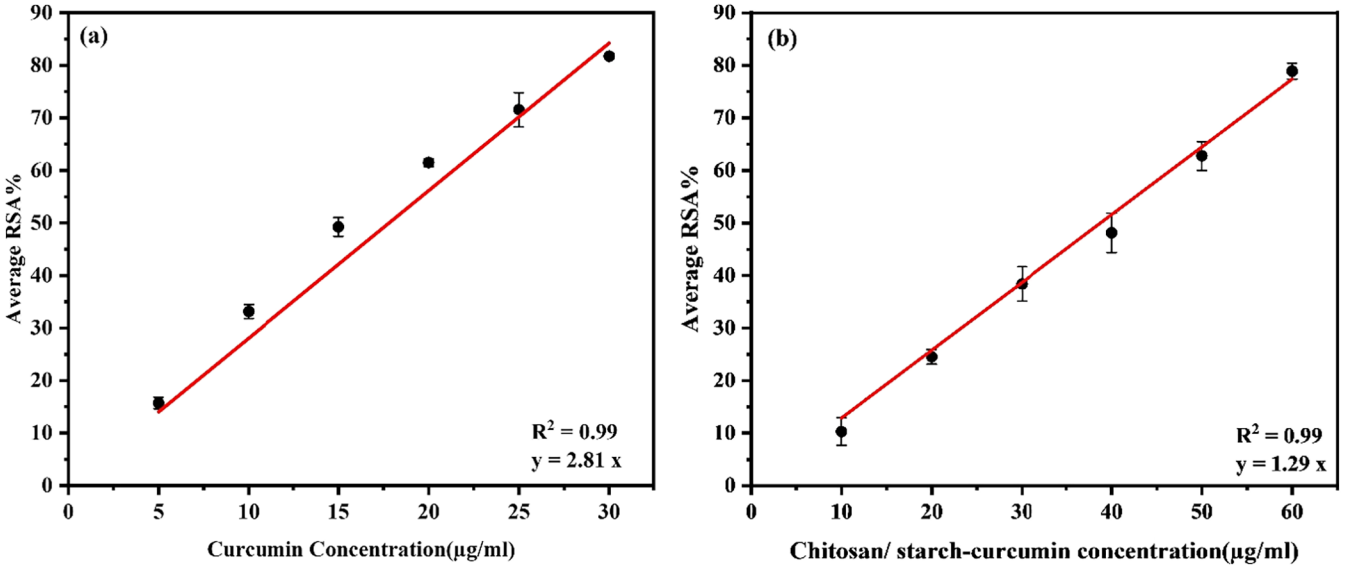

Figure 3. DPPH scavenging activities of (a) Curcumin extract (b) chitosan/starch-curcumin composite.

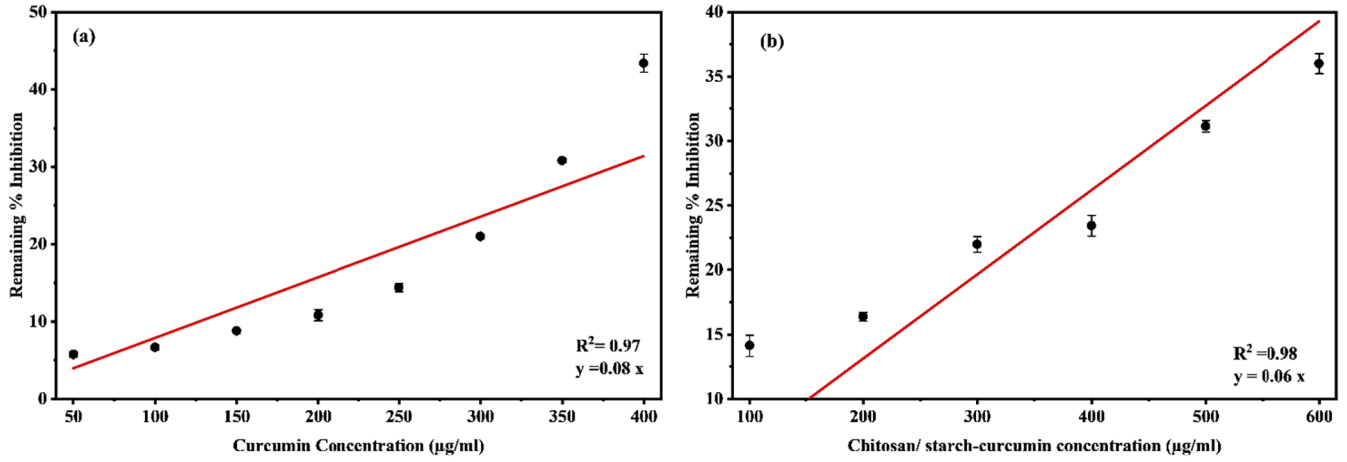

Figure 4. Remaining anti-inflammatory activity assay on (a) curcumin (b) chitosan/starch-curcumin composite.

indicating the potent antioxidant activity of the curcumin extract.

RSA% of the composite varied between 10.30 μg/mL and 78.88 μg/mL in the tested concentration range of 10−60 μg/mL, which was lower than the pure extract. The slightly decreased activity of the chitosan composite may result from the encapsulation of bioactive substances within the chitosan matrix, restricting their interaction with DPPH radicals. The IC_{50} of chitosan/starch-curcumin composite was 38.77 μg/mL. Based on the IC_{50} values of the composite, it can be inferred that the curcumin-loaded composite exhibits substantial antioxidant activity, protecting against the negative effects of free radicals. The sample's ability to scavenge free radicals (DPPH) increased with higher concentrations. The highest RSA% for chitosan/starch-curcumin was observed at 79 ± 1.52 at 60 μg/mL (Figure 3(b)). In contrast to reports where curcumin encapsulation improves DPPH scavenging ability by enhanced water dispersibility,[35,53] in the present study, the IC_{50} value of the curcumin extract was higher than that of the composite. Unlike the curcumin-loaded hyaluronic acid complexes[54] and curcumin-loaded chitosan/lecithin nanoparticles,[53] which has enhanced the activity by preventing curcumin aggregation, here, postcoating has created a more rigid barrier. Postcoating of the curcumin extract on the delivery system might have hindered the freely available curcumin for the reaction with DPPH, compared to the pure extract. This behavior is due to the reduced diffusion of curcumin from the dense chitosan/starch matrix and the availability of the free phenolic groups. Postcoating involved the formation of H-bonding and covalent linkages between the phenolic compounds, which are mainly responsible for its antioxidant activity, between curcumin and the polymeric system that can block these active sites freely available to scavenge the DPPH radicals. In polymer-based delivery systems that included chitosan, one phenolic group is required for covalent linkage to chitosan, which will temporarily attenuate curcumin's antioxidant capacity.[55] Nevertheless, the curcumin-loaded composite has also shown promising antioxidant potential while improving the bioavailability of the loaded drug.

The RSA% of the positive control (ascorbic acid) at 40 μg/mL was reported to be 94.9%, which is higher than that of the composite (48.1%). In comparison to the curcumin and composite, ascorbic acid demonstrated greater radical scaveng-

Downloaded from pubs.acs.org/acsodf/article-pdf/11/28/41667/6540397/acsomega.6c01210.pdf by guest on 15 August 2026

https://doi.org/10.1021/acsomega.6c01210
ACS Omega 2026, 11, 41667−41688

ing ability with an IC_{50} value of 4.21 μg/mL. The composite's RSA% was mainly attributed to the antioxidant potential of curcumin, which was grafted to the surface of the delivery system. However,[56,57] have reported that chitosan also possesses antioxidant activity. Tomida et al. have indicated that compared to high molecular weight chitosan, the antioxidant activity of low molecular-weight chitosan was stronger.[56] Alsharabasy A has found that low molecular-weight chitosan with a degree of deacetylation >90% exhibited higher scavenging activities[58] compared to a lower degree of deacetylation. However, the chitosan was not readily soluble in the methanol-based system used in the DPPH assay, preventing the assessment of the RSA% of the carrier. Since higher molecular weight chitosan was used in the synthesis of the delivery system, the components in the delivery system have not considerably contributed to the antioxidant potential of the drug composite. Therefore, results suggest that the chitosan/starch-curcumin composite is composed of substances, mainly curcumin, that can provide free radical hydrogen to neutralizes the odd electron of the ROS, which is responsible for the reactivity.

3.4. Anti-Inflammatory Assay

The antidenaturation assay of egg albumin was used to assess the anti-inflammatory properties of curcumin and chitosan/starch-curcumin composite (Figure 4(a,b)).

The assay is conducted based on the theory that anti-inflammatory drugs may stabilize protein structures and prevent denaturation, which is often associated with inflammation and tissue damage.[50] Curcumin has been identified in earlier research as a potent anti-inflammatory drug, and its action is mediated in many pathways that include interactions with more than 30 different proteins.[59] It is well-known for the inhibition of nuclear factor kappa B, which is related to inflammatory diseases.[60] Thus, the anti-inflammatory activity of the synthesized composite is mainly attributed to the presence of curcumin.

The remaining % inhibition activity of the curcumin and chitosan/starch curcumin composite in the concentration range of 100−600 μg/mL is shown in Figure 4(b). The IC_{50} values were calculated using the linear fit of the triplicated experimental data. Diclofenac sodium was used as the positive control. The higher inhibition activity exhibited at a lower concentration range (100−200 μg/mL) gradually declined at higher concentrations in both samples tested. Protein aggregation causes free curcumin's efficacy to decline at greater concentrations, despite its enhanced action at 100−200 μg/mL. The composite maintains more stable activity across a broader range compared to that of the free curcumin. While the composite underperforms free curcumin at low doses due to restricted immediate availability, it avoids the high-dose self-antagonism seen with free curcumin. Excess curcumin promotes nonspecific aggregation of egg albumin, lowering the particular stability of the protein structure. But it is important to highlight that the activity of the % inhibition has been reduced with the increased concentration of both compounds. Composite material has depicted a similar level of anti-inflammatory activity because of the anti-inflammatory activity of the loaded curcumin. The activity can be explained *via* the postcoating process of curcumin. The concentration-dependent reduction in the % inhibition activity is attributed to the increased turbidity caused by the protein-polyphenol interactions with the increase of curcumin concentration.[61] Curcumin has been coated onto the surface of the chitosan/starch delivery system in the synthesis procedure through hydrogen bonding with its phenolic−OH groups and covalent connections. This conjugation limits curcumin's rapid availability at low doses, thereby reducing its action. The same coating offers controlled release at high doses, avoiding the saturation that leads to the aggregation and loss of effectiveness of free curcumin. As a result, the composite avoids high-dose self-antagonism while exhibiting lower activity in lower concentrations. Results suggest that the ability of curcumin to inhibit egg albumin denaturation may exhibit dose-dependent effects, with lower concentrations of curcumin providing greater protection against denaturation. Similar results were documented in a previously released study.[59] The study, which has been done by Belma et al., has proven that curcumin is highly anti-inflammatory compared to acetylsalicylic acid, known as aspirin, a widely used non-steroidal anti-inflammatory drug.[59]

Nonsteroidal anti-inflammatory medications like curcumin can stop the denaturation of egg albumin by stabilizing the lysosomal membrane.[16] This membrane-stabilizing action may partially inhibit egg albumin denaturation in the experiment. Curcumin interacts with egg albumin to create complexes through noncovalent interactions. These interactions help curcumin attach to egg albumin molecules, which may prevent denaturing chemicals from penetrating the protein surface and, hence, ultimately prevent denaturation. The potential of the prepared chitosan/starch-curcumin composite has demonstrated the ability to prevent protein denaturation and, therefore, can be improved as a natural anti-inflammatory therapeutic drug.

3.5. Antibacterial Activity

Antibacterial activity of curcumin has been observed in a broad spectrum of antifungal, antivirus and antibacterial agents of both Gram-positive and Gram-negative strains, including *P. aeruginosa*, *S. aureus*, *Bacillus subtilis*, *Bacillus cereus*, *E. coli*, and *Bacillus coagulans*.[62] In bacterial cells, curcumin causes oxidative stress, DNA damage, and cell death *via* apoptosis. Curcumin contributes to bacteriostatic effects by blocking the bacterial DNA damage repair pathway. The antibacterial mechanism of action of curcumin includes bacterial quorum sensing, a specific communication process mediated by biochemical signals that regulate cell density and microbial behavior, and damage to the cell wall or membrane and interfering with cellular processes by targeting DNA and proteins.[5]

The most widely accepted antibacterial action for chitosan is attaching chitosan to the negatively charged bacterial cell wall, which disrupts the cell and changes the permeability of the membrane. Lower molecular weight chitosan can penetrate the cell wall by passing through pores, causing the cell wall to collapse, and then bind to DNA. This process inhibits DNA replication and ultimately results in cell death.[63] Chitosan's NH_2 group, which can be protonated to NH_3^+ and readily form electrostatic interactions with anionic groups of microbial cell membranes, leading to the leakage of proteinaceous and other intracellular constituents of the microorganism. According to Shehabeldine et al., the degree of deacetylation is correlated with the polycationic chitosan charge.[64] Strong electrostatic interaction, which is a key component of antibacterial activity, is produced due to the higher positive charge densities of protonated amino groups ($-NH_3^+$), which

Downloaded from pubs.acs.org/acsodf/article-pdf/11/28/41667/6540397/acsomega.6c01210.pdf by guest on 15 August 2026

https://doi.org/10.1021/acsomega.6c01210
ACS Omega 2026, 11, 41667−41688

are attracted to the negatively charged bacterial surface, causing agglutination of chitosan, or an increase in the microbial wall permeability, which ultimately triggers the release of the internal components. By attaching to microbial DNA, chitosan can prevent the creation of mRNA and proteins.

In the current study, starch was used as a part of the delivery system, which increases the bioavailability of curcumin to result in better control of the drug release. It was observed that starch did not contribute to the antibacterial activity of the composite or the curcumin-loaded composite, significantly.[65] Although the antibacterial activity of chitosan and curcumin has been studied extensively, the antibacterial activity of the curcumin-loaded chitosan/starch composites has not been studied over a broad range of Gram-negative and positive bacterial strains. Thus, the study provides insightful information about the antibacterial activity and possible mechanisms of action of the curcumin composite that can be used in potential pharmaceutical applications. A summary of the reported antibacterial mechanisms has been depicted in Figure S4.

The antibacterial activity of the synthesized materials was assessed using the agar well diffusion method. The impact of the curcumin extract, chitosan/starch composite and curcumin-coated chitosan/starch composite on the inhibition of bacteria was tested on both Gram-positive and Gram-negative bacterial strains, including *S. aureus*, *P. aeruginosa*, *K. pneumoniae* and *E. coli* under varying concentrations of 2.5, 5,10 and 20 mg/mL. The test samples, including the curcumin extract, biopolymer composite, and drug composite, should diffuse through the solid agar media to interact with the bacterial cell walls to cause antibacterial activity.

The chitosan/starch composite showed inhibition zones only for *P. aeruginosa*, resulting in zones of inhibition of 11.66 ± 0.78 mm, 8.89 ± 0.4 mm, 9.00 ± 0.38 mm and 10.00 ± 0.51 mm for 2.5 mg/mL, 5 mg/mL, 10 mg/mL, and 20 mg/mL concentrations, respectively. The highest zone of inhibition was reported with a 2.5 mg/mL concentration. Interestingly, the zone of inhibition reported for the chitosan biopolymer was 11.12 ± 0.78, 7.98 ± 0.40, 8.98 ± 0.38, and 10.0 ± 0.51 for the above-mentioned concentration range. Therefore, it is evident that the reported antibacterial activity of the chitosan/starch carrier against the *P. aeruginosa* is attributed to the antibacterial activity of chitosan. However, the chitosan/starch composite or chitosan biopolymer did not show any antibacterial effect against other bacterial strains tested, including *S. aureus*, *E. coli* and *K. pneumoniae*, in the tested concentration range. Starch did not exhibit antibacterial activity against any of the bacterial strains tested in the current study (Figure S5). Shehabeldine and Hasanin et al., proved that hydrolyzed starch exhibited no antibacterial activity against either Gram-positive bacteria or Gram-negative bacteria, validating these results.[64] Therefore, the reported antibacterial zones have resulted from the antibacterial activity of chitosan. Chitosan was not reported to exhibit significant antibacterial activity against Gram-positive *S. aureus* because both bacterial cells and chitosan have positive charges that repel each other and keep them away from interacting closely.[66] Furthermore, the positive charges on bacterial cells and chitosan in the case of Gram-positive bacteria have a repelling effect that prevents them from coming into close contact.[44] The chitosan/starch composite has shown inhibition zones only in *P. aeruginosa* and not in other Gram-negative microorganisms. According to Ardean et al., chitosan's antibacterial activity was shown to be prominent against Gram-negative bacterial strains. However, this activity could be varied due to several reasons, including molecular weight, degree of deacetylation, source and concentration.[67] The antibacterial activity of chitosan is limited due to its poor aqueous solubility, limiting the use of this natural biopolymer as an antibacterial agent. In the present study, higher molecular weight chitosan was used as the delivery system for curcumin coupled with starch, which limits its activity toward the Gram-negative bacterial strains significantly. Because the antibacterial mechanism of chitosan is based on its ability to adhere and absorb into cell surfaces, which results in cell leakage causing the change in membrane permeability Huszczynski et al. has indicated that *P. aeruginosa* has a more permeable outer membrane with fewer lipopolysaccharides accelerating the cellular uptake of chitosan, while the cell wall structure of *E. coli* and *K. pneumoniae* consist with thicker lipopolysaccharide layers[68] limiting the cellular uptake of the composite and the curcumin loaded chitosan/starch delivery system. This limits the antibacterial activity of the composite and the composite-loaded curcumin against *K. pneumoniae* and *E. coli*.

Curcumin has exhibited effective antibacterial activity against the Gram-positive *S. aureus* and Gram-negative *P. aeruginosa* bacterial strains. The diameter of the zones of inhibition against *P. aeruginosa* by curcumin extract was reported to be 14.00 ± 1.17 mm, 13.55 ± 0.9 mm, 12.11 ± 0.29 mm, and 10.11 ± 0.44 mm for 2.5, 5, 10, and 20 mg/mL concentrations, respectively. The results indicated a dose-dependent decrease in the zone of inhibition at higher concentrations of the sample tested, suggesting that higher concentrations of curcumin were associated with reduced antimicrobial activity for *P. aeruginosa*. The zones of inhibition for curcumin extract against *S. aureus* were 12.33 ± 1.17 mm, 12.89 ± 1.16 mm, 14.22 ± 0.48 mm and 15.56 ± 0.29 mm for 2.5, 5, 10, and 20 mg/mL concentrations, respectively. The antibacterial activity of curcumin against *S. aureus* increased with increasing curcumin concentration, indicating a dose-dependent increment in the antimicrobial activity. The highest zone of inhibition for curcumin was shown as 15.56 ± 0.29 mm for 20 mg/mL for *S. aureus*. In contrast, curcumin extract has not shown any zone of inhibition in the tested concentrations for *E. coli* and *K. pneumoniae*, which are reported as strong Gram-negative bacterial strains.

Curcumin has shown distinct better effectiveness against Gram-positive bacteria than Gram-negative bacteria, which complies with prior research.[69,70] Adamczak et al. reported that their results have shown a significantly higher activity of curcumin against Gram-positive than Gram-negative bacteria.[69] The differences in the makeup and structure of microbial cell walls are assumed to be the reason why curcumin and other natural compounds have a stronger effect on *S. aureus*. Gram-positive bacteria lack an outer membrane, but their cells are encased in a thick layer of peptidoglycan that contains an extra class of lipoteichoic acids (LTA). It facilitates the passage of hydrophobic molecules through the cell wall more easily. Curcumin functions as an antibacterial agent against Gram-positive bacteria by blocking the bacterial surface protein sortase A and preventing cell attachment to the binding protein, fibronectin of *S. aureus*. Furthermore, curcumin inhibits the release of Penicillin-binding protein 2, a protein from *S. aureus*, which is encoded by the mecA gene and disrupts the process of protein synthesis by causing damage to

Downloaded from pubs.acs.org/acsodf/article-pdf/11/28/41667/6540397/acsomega.6c01210.pdf by guest on 15 August 2026

https://doi.org/10.1021/acsomega.6c01210
ACS Omega 2026, 11, 41667−41688

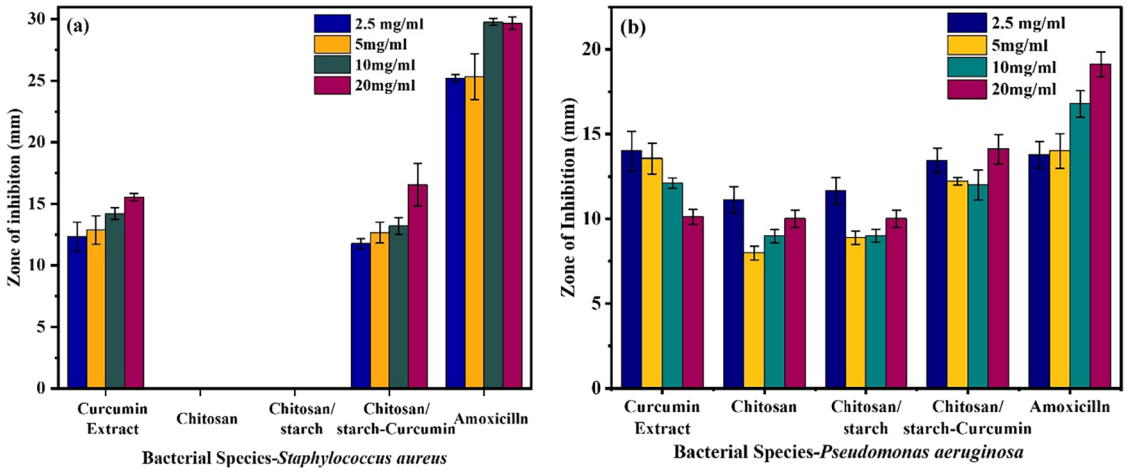

Figure 5. Antibacterial activity of curcumin extract, chitosan/starch composite, curcumin loaded chitosan/starch composite and positive control against (a) *S. aureus* and (b) *P. aeruginosa*.

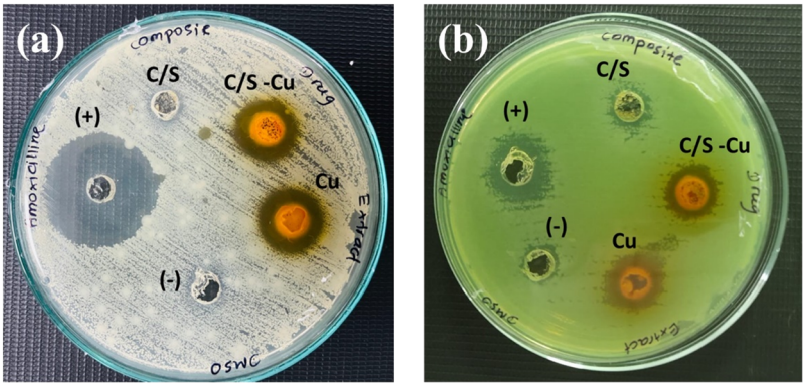

Figure 6. Well diffusion results of the tested compounds against (a) *S. aureus* and (b) *P. aeruginosa*.

RNA.[5] Additionally, curcumin generated lipid peroxidation, enhanced DNA breakage, and impacted the metabolism of L-tryptophan in Gram-positive *S. aureus* but not in Gram-negative *E. coli*.[62]

Due to variations in bacterial membrane structure, efflux mechanisms, and particular virulence targets, curcumin's antibacterial effectiveness against Gram-negative bacteria varies quite significantly.[62,70] As mentioned in Górski et al, *K. pneumoniae* isolates that produce carbapenemase exhibit significantly broad-spectrum antibiotic resistance, including curcumin.[70] RecA protein expression, which drives apoptotic-like death processes in bacteria, was upregulated at the genetic level by curcumin. Dai et al. demonstrate that curcumin resistance was seen in *E. coli* RecA knockouts, which proves that curcumin-induced cell death in *E. coli* is dependent on apoptotic pathways.[71] *P. aeruginosa* has a less restrictive outer membrane, as mentioned in Dai et al., *P. aeruginosa* shows antibacterial activity against curcumin by preventing the synthesis of the quorum-sensing-dependent components, including the formation of alginate and exopolysaccharides.[71] Therefore, the results are consistent with the previous studies where curcumin's antibacterial mechanism was highly effective against Gram-positive *S. aureus*, while exhibiting moderate antibacterial activity against gram-negative *P. aeruginosa*.

Between *P. aeruginosa* and *S. aureus*, *S. aureus* was more susceptible to the antibacterial activity of curcumin-loaded chitosan/starch composite. The zones of inhibition that were reported for curcumin-loaded chitosan/starch composite against *P. aeruginosa* were 13.44 ± 0.73 mm, 12.22 ± 0.22 mm, 12.00 ± 0.88 mm and 14.11 ± 0.87 mm, while *S. aureus* showed zones of inhibition of 11.78 ± 0.4 mm, 12.67 ± 0.84 mm, 13.22 ± 0.68 mm and 16.56 ± 1.72 mm at 2.5,5,10 and 20 mg/mL concentrations, respectively. The zones of inhibition depicted for *S. aureus* have increased with increasing concentration, indicating enhanced antimicrobial activity at higher concentrations. This finding is consistent with the antibacterial activity of curcumin as discussed above. Therefore, the antibacterial activity of *S. aureus* against curcumin is mainly attributed to the antibacterial mechanism of curcumin. However, grafting curcumin onto the surface of the delivery systems has positively affected the antibacterial action at higher concentrations. Conversely, the reported inhibition zones for the antibacterial activity of curcumin-loaded chitosan/starch composite for *P. aeruginosa* have decreased with the increment of the concentration, except for the 20 mg/mL concentration, where it showed an enhanced antibacterial effect. In both bacterial strains, the drug composite at 20 mg/mL exhibited an enhanced synergistic antibacterial effect, where the diameters of the reported zone of inhibition are larger compared to the curcumin extract or the chitosan/starch composite alone. The zone of inhibition (mm) reported for curcumin extract at 20 mg/mL was 15.56 ± 0.29 mm and 10.11 ± 0.44 mm for *S. aureus* and *P. aeruginosa*, respectively. Whereas at the same concentration, the reported zones of inhibition (mm) for the

Downloaded from pubs.acs.org/acsodf/article-pdf/11/28/41667/6540397/acsomega.6c01210.pdf by guest on 15 August 2026

https://doi.org/10.1021/acsomega.6c01210
ACS Omega 2026, 11, 41667−41688

curcumin-loaded drug composite were 16.56 ± 1.72 mm and 14.11 ± 0.87 mm, for the same bacterial strains. The result of *S. aureus* for the curcumin extract was consistent with a prior investigation by Li et al. on curcumin antimicrobial efficacy.[72] No zones of inhibition were reported for the curcumin-loaded chitosan/starch composite against the *E. coli* and *K. pneumoniae* in the tested concentration range, similar to the results reported for the curcumin extract and the chitosan/starch composite.

Amoxicillin was used as the positive control. It showed higher zones of inhibition than curcumin, chitosan/starch composite, and curcumin-loaded chitosan/starch composites against all the test microorganisms at 2.5, 5, 10, and 20 mg/mL concentrations. The highest zone of inhibition for Amoxicillin was recorded against *E. coli* with a zone of 40.44 ± 0.22 mm at 20 mg/mL.

The results shown in Figure 5 show that the Curcumin-loaded chitosan/starch composite showed greater inhibitory activity to the Gram-positive strain of *S. aureus* as well as Gram-negative strains of *P. aeruginosa*. Figure 6 represents the inhibition zone for the respective bacterial strains on agar plates. These findings are similar to the results reported by Jahanizadeh et al., where the Gram-positive *S. aureus* has demonstrated better antibacterial activity against curcumin-loaded chitosan/carboxymethyl starch/montmorillonite, and Gram-negative strains of *P. aeruginosa* have demonstrated efficient antibacterial activity for chitosan-cross-linked curcumin-tannic acid biocomposites, respectively.[73]

For instance, both curcumin-loaded chitosan/starch composite and curcumin extract have not shown a zone of inhibition diameter in *K. pneumoniae* and *E. coli*. It is commonly known that Gram-positive bacteria are typically more sensitive to antibiotics than Gram-negative bacteria, even though both types have a stronger peptidoglycan coating in their cell walls.[74] The outer membrane of Gram-negative bacteria, which is made up of a lipid-rich structure that serves as a barrier to many antimicrobial drugs, is the main cause of this increased resistance. As a result, when tested against the Gram-negative bacterium *K. pneumoniae* and *E. coli*, curcumin and the curcumin-loaded chitosan/starch composite material showed no zones of inhibition within the tested concentration range.[75] This resistance can be attributed to the structural characteristics of the *E. coli* outer membrane, which contains outer membrane proteins (OMPs) that function as selective channels, thereby regulating the entry of molecules into the bacterial cells.[44] According to Azucena et al., this resistance of *E. coli* to curcumin may stem from strain-specific genetic factors.[76] Through RecA-mediated mechanisms, curcumin causes *E. coli* to exhibit responses resembling apoptosis. Curcumin is ineffective in strains missing RecA because they do not exhibit DNA fragmentation or phosphatidylserine exposure.[71]

The specific composition and quantity of the composite, as well as the technique used to test the antibacterial activity, may affect how effectively curcumin-loaded chitosan/starch composite inhibits the growth of *K. pneumoniae*. It is well-recognized that bacteria, such as *K. pneumoniae*, can have a variety of enzymes, such as β-lactamases or carbapenemases that support their resistance and ability to survive. These enzymes could be involved in the modification or breakdown of foreign materials, including curcumin. According to Yada et al.,[77] some strains utilize active transport systems to expel curcumin.

In the present study, the curcumin-loaded chitosan/starch composite was shown to exhibit enhanced antibacterial activity against *S. aureus* and *P. aeruginosa* at 20 mg/mL, while maintaining prominent activity across the tested concentration range of 2.5−20 mg/mL. These findings were aligned well with the reported literature for individual components in the delivery system. However, the study concluded the novel findings for the enhanced antibacterial activity against the tested bacterial species. Therefore, loading curcumin into a chitosan/starch delivery system can enhance the antibacterial activity of the curcumin extract, providing benefits for therapeutic applications.

3.6. *A. cepa* Cytotoxicity Assay

Mitotic index of the treated samples was calculated to further evaluate the cytotoxic effects of the samples on onion root tip cells. As presented in Table 2, the negative control exhibited a normal MI of 52.5%. At 2.5 mg/mL, all treatments showed slightly reduced MI values compared to the negative control, but still within a range indicative of active cell division. As indicated by Antosiewicz, a MI% value below 22% compared to the negative control indicates the possible cytotoxicity, whereas a decline below 50% indicate sublethal effects, and is referred to as the cytotoxic limit value.[78] Although within the accepted range, at 20 mg/mL, a noticeable reduction in MI was observed for all samples compared to the value reported at 2.5 mg/mL. Additionally, at 2.5 mg/mL, all three samples exhibited a good distribution of cells across all four mitotic phases (prophase, metaphase, anaphase, and telophase), indicating normal progression through the cell cycle. On the contrary, at 20 mg/mL, a clear shift in phase distribution was observed. In all three treatment groups at 20 mg/mL, the majority of mitotic cells were arrested in prophase at the time of cell fixation. Cells in metaphase, anaphase, and telophase were markedly reduced or nearly absent in the test samples at 20 mg/mL. Prophase cells were very prominently visible, but subsequent stages were scarce, suggesting a block in mitotic progression at the prophase-to-metaphase transition. The root tip cells in the mitotic phase, which were observed under the 400× magnification, are indicated in Figure 7(a−f).

Table 2. Mitotic Index in Control and Treatment Concentrations

sample/treatment	MI % (2.5 mg/mL)	MI% (20 mg/mL)
Curcumin	36.87 ± 9.45	26.57 ± 2.08
Chitosan/starch	40.67 ± 5.51	26.6 ± 1.85
Curcumin-chitosan/starch composite	41.8 ± 8.89	32.87 ± 3.55
Negative control	52.5 ± 4.51	

In the positive control ($K_2Cr_2O_7$), root tip cells showed no stained mitotic cells. The nuclei were extremely condensed and hyperchromatic, with no visible chromosomal structures. Further, the cell walls of some cells in the root tips were completely damaged, which promotes the elimination of the nucleus from the cell (Figure 7(g,h)). No cells were observed in prophase, metaphase, anaphase, or telophase, indicating complete arrest of the cell cycle before mitotic entry.

When the results are compared with the general toxicity study (root elongation), which is reported in the Supporting Information section 2.5 (Figure S6), a reduction in root length could occur without actual cell cycle arrest. Interestingly, all the test samples that indicated better root elongation (2.5 mg/

Downloaded from pubs.acs.org/acsodf/article-pdf/11/28/41667/6540397/acsomega.6c01210.pdf by guest on 15 August 2026

https://doi.org/10.1021/acsomega.6c01210
ACS Omega 2026, 11, 41667−41688

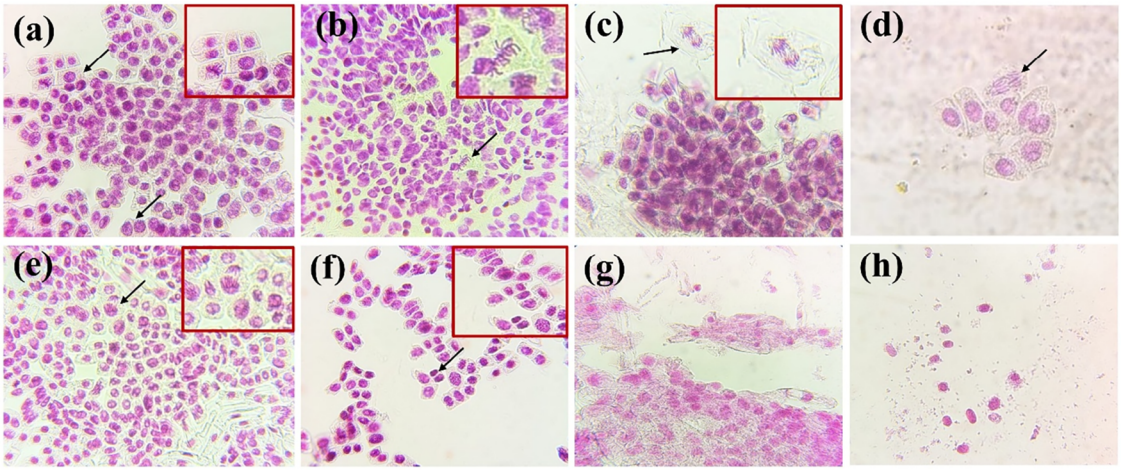

Figure 7. Microscopic appearance of cells in mitosis in *A. cepa* root tip meristematic region (a) prophase; (b) metaphase; (c−e) anaphase; (f) telophase; (g, h) cells of positive control with damaged cell membrane.

mL) had MI above 22%, suggesting lower cytotoxic effects. Importantly, at this concentration, all three samples maintained a normal distribution of cells across prophase, metaphase, anaphase, and telophase. This indicates that although the rate of cell division was somewhat reduced (compared to the negative), the cell cycle machinery remained functional, and cells could complete mitosis. At 20 mg/mL, all three treatments caused marked root growth inhibition (>47% reduction) and substantially reduced MI values (26−33%). More critically, the cell cycle was arrested predominantly at prophase, with very few cells progressing to metaphase, anaphase, or telophase. However, cells had entered the mitotic division at the time of observations, and the rate of progression through mitosis was slower compared to the lower concentration value. Thus, the combined results of the general toxicity and cytotoxicity assay suggest that the synthesized compounds are not cytotoxic at lower concentrations (2.5 mg/mL) but can delay the mitotic division at higher concentrations.

Although the mitotic index analysis and the *A. cepa* root elongation test offer useful initial insights into the toxic and cytotoxic potential of synthesized samples, these assays have several limitations. As a result, the current study should be regarded as an initial inquiry that offers basic cytotoxicity information.

3.7. Drug Release Studies

Covalent and noncovalent interactions interact dynamically during the composite synthesis, defining its three-dimensional structure and functional characteristics. The amine groups ($-NH_2$) of chitosan and the aldehyde groups (−CHO) of glutaraldehyde primarily undergo a Schiff base reaction to create covalent imine (C═N) bonds, facilitating the cross-linking of chitosan chains. This covalent framework is additionally reinforced and made flexible by a network of hydrogen bonding interactions. These bonds include glycerol and the hydroxyl groups of starch, as well as among the functional groups of chitosan, starch, PVA, and glycerol, which in turn improve the material's physical stability and flexibility. Curcumin is physically loaded within this porous, cross-linked network, with its retention regulated by hydrogen bonding and hydrophobic interactions with the polymer matrix, rather than through covalent attachment, helping to preserve its bioactivity. The proposed chemical reactions are illustrated in Figure S7, whereas the interactions with the cell membrane and the cellular fate of the drug-loaded carrier are shown in Figures S8 and S9, respectively.

To assess the impact of the physiological conditions on the release of curcumin from chitosan/starch polymer composite, the pH and the ionic strength of the media were changed systematically. pH of the release media was varied between pH 1−pH 8, while the NaCl concentration was varied from 0.1 M−0.5 M to change the ionic strength. As the oral and IV administrations are focused on in the current study, the pH range was selected to be inclusive of the pH gradient present in the GI tract and the pH of the peripheral blood (pH 7.4). For the oral dosage forms, the stomach is the first place where the disintegration and dissolution take place because the delivery time of the drug composite through the oral cavity and esophagus is relatively short. Gastric juice consists of a strong acidic pH range between 1.0 and 2.0. The intestines are the major absorption site for drugs, and the pH increases from pH 6 in the duodenum to pH 7−8 in the distal part of the ileum.[79] Additionally, the release profile of curcumin, which is a proven anticancer agent, was studied in lower pH values (pH 5.5−6.8). The pH values of the extracellular matrix of the malignant tissues are reported to be lower than the normal extracellular pH (7.4) because of elevated glycolysis for ATP production, even at normal oxygen levels. Moreover, the ionic strength of the extracellular matrix is governed by the concentration of ions, including K^+, Na^+, Ca^{2+} and H^+. These concentrations are altered in malignant tissues, specifically the concentration of Na^+ ions.[80] It is reported that in most tumor types, including brain,[81] breast,[82] prostate and uterine cancer,[83] extracellular and intracellular Na^+ concentrations are significantly higher than in normal tissues. Hence, in order to assess the differences in the release profile of curcumin under varied Na^+ concentrations, the above range was selected. Since curcumin tends to aggregate in media with higher ionic strength (500 mM to 1000 mM) due to the strong van der Waals forces predominating over the electrostatic repulsion forces ionic strength was maintained below 500 mM.[84] Therefore, evaluating the behavior of the release mechanism under varying physiological conditions could provide insights into pH-responsive controlled release and site-specific action of the therapeutic agent.

Downloaded from pubs.acs.org/acsodf/article-pdf/11/28/41667/6540397/acsomega.6c01210.pdf by guest on 15 August 2026

https://doi.org/10.1021/acsomega.6c01210
ACS Omega 2026, 11, 41667−41688

3.7.1. Loading Efficiency of Curcumin

The encapsulation efficiency of curcumin in the chitosan/starch biopolymeric delivery system was calculated using the curcumin calibration curve (Figure 8). The concentration of

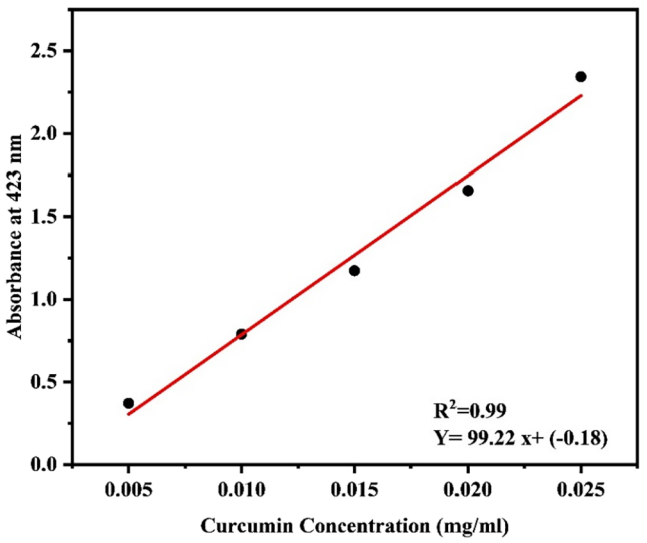

Figure 8. Calibration curve of curcumin.

unbound curcumin in the polymeric delivery systems was derived using the linear regression equation of the resulting calibration curve. LE% was calculated using eq (3). The Curcumin loading efficiency in the chitosan/starch composite was reported to be in the moderate range, with a value of 51.0%.

During the synthesis of the drug carrier, cross-linkers like sodium tripolyphosphate were not used, and therefore, the composite lacks ionic or covalent interactions with the weakly acidic, hydrophobic curcumin. Water-in-Oil-in-Water (W/O/W) emulsification can enhance the EE% of hydrophobic therapeutic agents, as reported in the literature. However, the recorded value for EE% is considerably moderate compared to advanced delivery systems which have used this approach. A double emulsion approach to load curcumin onto a pH-sensitive nanocomposite consisting of chitosan/gelatin/carbon quantum dots has been used by Ostovar et al.[85] with an EE% of 46.75%. Rajabzadeh-Khosroshahi et al.[86] has reported that incorporating graphitic carbon nitride into the pH-sensitive nanocarrier system composed of chitosan/agarose and entrapping curcumin using W/O/W emulsification can enhance the EE% from 42% (chitosan/agar) to 54%.

Drug encapsulation efficiency was considered when converting the absorbance data into the cumulative drug release percentage (CDR%). At lower pH values (1.0−2.5), curcumin release was relatively higher, showing a burst effect due to the protonation of NH_2 groups of the chitosan that weakens the drug-polymer interactions.[87] In the moderate pH levels (4.0−6.7), the release was comparatively reduced compared to acidic conditions, where the chitosan matrix has stabilized, slowing down the diffusion rate, indicating a sustained release. Based on the CDR% % data, curcumin release was highest in the media with pH 7.4, where the curcumin solubility and the matrix stability were well maintained. However, in alkaline conditions, the release of curcumin was reported to be lowest because of the deprotonation of the chitosan matrix.[88] This leads the polymer to be less hydrophilic, and it entraps the curcumin inside the matrix while accelerating the degradation of curcumin. CDR% in the media with changing [NaCl], curcumin release was reduced with the increment of the Na^+ concentration, showing the highest release rates at 0.1 M [NaCl]. High ionic strengths cause salting-out effects, making the hydrophilic chitosan polymer less accessible to interact with the media.[89] Curcumin tends to be physically trapped in the tightened polymer, slowing the release. However, the natural biological fluids tend to maintain a Na^+ concentration of around 135−145 mM/L in the extracellular fluid. The results of the study reveal that the release of curcumin in the media with pH 7.4 and 0.1 M NaCl concentration is higher with a sustained release, allowing the polymer matrix and coated curcumin to be stable under these conditions. This suggests the curcumin-loaded chitosan/starch biopolymeric delivery system is stable for oral and IV delivery.

3.7.2. Storage Stability of the Composite. The goal of this stability study was to determine whether intact curcumin remains loaded on the composite after extended storage. After 6 months, the free curcumin concentration in the supernatant increased substantially (from 2.45 mg/mL to 3.27 mg/mL). Further, the loading efficiency dropped from 51.0% to 34.58%, representing a loss of 32.2% relative reduction in loaded curcumin. This reduction could result from physical release (leaching) of curcumin from the composite, chemical degradation of curcumin, or a combination of both mechanisms.

This formulation's curcumin-chitosan-starch interactions are all completely noncovalent (van der Waals forces, hydrophobic interactions, and hydrogen bonds). Without chemical cross-linking or covalent attachment, total retention over six months in an aqueous medium is not feasible due to the intrinsic dynamic nature of such reversible interactions. Thus, 65.4% release over 6 months is in line with what would be expected from a non-cross-linked polysaccharide matrix.

3.7.3. Drug Release Kinetics. Cumulative drug release % data was fitted into six drug release kinetic models, namely, Zero-order, First-order, Higuchi, Hixson−Crowell (HC), Korsemeyer−Peppas (KP) models, and Peppas-Sahlin (PS) kinetic models, considering the first 60% of release. Fitting the release data to the mathematical equations results in model parameters that are relevant to each model and the R^2 between the experimental data and the model fit. The model parameters can differ according to the model considered; however, the release constant (k), which is related to the release rate of the drug, is considered in all the models. This k value is used to compare the release rate and optimize the release profile to match the intended outcomes. The R^2 value was used to determine the best-fitted model to explain the release mechanism of curcumin from the chitosan/starch biopolymeric delivery system. Tables S3 and S4 summarize the model parameters of the mathematical models, indicating the release behavior of curcumin under varying physiological conditions along with the R^2 value for each model. Models with the $R^2 \geq 0.99$ were selected to elucidate the drug release mechanism. Korsmeyer Peppas model and Peppas Shalin model met the above criteria for all the release media compositions, and the Higuchi model was also reported to have a higher R^2 in most of the media compositions. Zero order, first order and Hixson-Crowell models exhibited $R^2 < 0.98$ for the tested media compositions, and hence those mathematical models were not taken into account when interpreting the release mechanism of curcumin from the biopolymer.

Downloaded from pubs.acs.org/acsodf/article-pdf/11/28/41667/6540397/acsomega.6c01210.pdf by guest on 15 August 2026

https://doi.org/10.1021/acsomega.6c01210
ACS Omega 2026, 11, 41667−41688

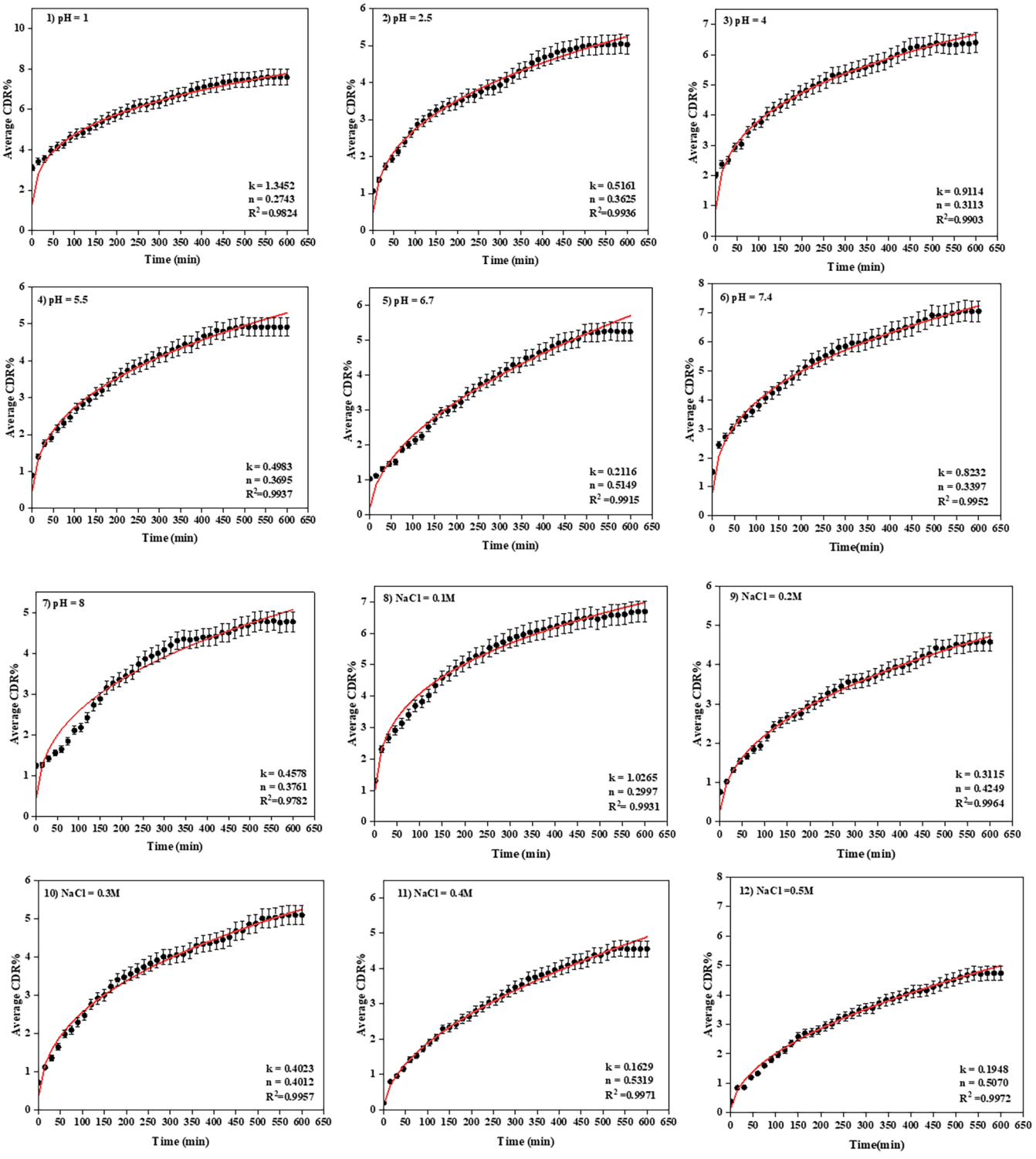

Figure 9. Fitted %CDR data for Korsmeyer−Peppas model of the drug composite under varying media conditions; (1−7) pH and (8−12) ionic strength.

In mechanistic models, the diffusivity concept is incorporated along with Fick's law. Fick's first law elaborates the steady-state diffusion where the flux flows according to the concentration gradient and the magnitude is proportional to the concentration gradient. Whereas the second law predicts the effect of diffusion on varying concentrations. Drug delivery methods usually fall into one of two categories: Fickian or non-Fickian solute diffusion. Fickian diffusion occurs when the solvent diffusion time is longer than the polymer relaxation time. Non-Fickian diffusion, which cannot be predicted using Fick's diffusion rules, will take place when relaxation time predominates the diffusion time.[90]

The "power law" or Korsmeyer-Peppas equation is a diffusion-based semiempirical technique used to indicate the primary delivery mechanisms involved in the release, either by swelling or diffusion. Drug release in hydrogel and other

Downloaded from pubs.acs.org/acsodf/article-pdf/11/28/41667/6540397/acsomega.6c01210.pdf by guest on 15 August 2026

https://doi.org/10.1021/acsomega.6c01210
ACS Omega 2026, 11, 41667−41688

polymeric systems could be accurately represented by this equation. This model is helpful when dealing with complex controlled process mechanisms, like when multiple release mechanisms are coupled or when Case II transport (non-Fickian) and active principle diffusion (Fickian diffusion) are combined. The release exponent (n) defines the release mechanism of the therapeutic agent in the KP model. When n = 0.43, it indicates pure Fickian diffusion, while n < 0.43 indicates quasi-Fickian diffusion. For values in the range 0.43 < n < 0.85, the mechanism shows non-Fickian diffusion, which is characterized by a combination of diffusion and swelling control. Additionally, for n = 0.85, the model matches case II transport, which is mostly governed by gel swelling.[91] A comprehensive understanding of the different drug release patterns observed in polymeric systems is provided by this theoretical framework.

Figure 9 demonstrates the nonlinear kinetic model fits of the KP model according to the parameters varied, and Tables S3 and S4 indicate the model parameter values, including n and release constant (k_P). R^2 values for the KP model are within the range of 0.99−1.0 for the tested release media; hence, the release mechanism can be explained using the Fickian diffusion principle. Release exponent (n) values range between 0.27−0.38 for the release of curcumin from the polymer matrix under different pH media compositions, suggesting that quasi-Fickian diffusion governs the release mechanism. This mechanism is similar to Fickian diffusion but considers the effect of swelling and relaxation of the polymer matrix.[92] Thus, the process deviates from perfect Fickian behavior due to these variables, indicating that there are other factors at play besides concentration gradients. Instead, molecule mobility is influenced by a system of diffusion and other processes. This implies that, in addition to the active ingredient's diffusion, drug release is aided by the relaxation of polymer chains in chitosan or carrier surface degradation. Chitosan, the major component responsible for the release of curcumin from the polymer, is a pH-sensitive polymer, where it remains protonated (NH_3^+) in acidic media.[93] It limits the swelling due to the electrostatic repulsion, but a slight relaxation can occur due to hydration. In the media with the pH range of 1−5.5, diffusion predominates with minor relaxation. In contrast, the n value reported for the KP model fir of the pH 6.7 media (n = 0.52) is in the range of 0.43 < n < 0.85, suggesting the non-Fickian diffusion mechanism controls the curcumin release. In the media with pH 6.7, chitosan was deprotonated to NH_2 partially (pH > pK_a) and exhibited optimal swelling with the water uptake. Maximum swelling can be expected to occur near the pK_a value. Here, anomalous transport occurs where the diffusion and polymer relaxation equally contribute to the drug release.[94] In the alkaline pH (7.4−8), the Quasi-Fickian release mechanism reoccurs, with the complete deprotonation of chitosan, reducing the water uptake. This leads to reducing the swelling at alkaline pH, given the poor solubility of chitosan in higher pH values and the weak electrostatic repulsion between chitosan chains with the deprotonation.[93] Therefore, diffusion with slight relaxation/erosion governs the release under alkaline conditions.

Ionic strength impacts the swelling of the chitosan, a positively charged component in the delivery system, which ultimately contributes to the alterations in the release mechanism. Quasi-Fickian diffusion predominates in the media with ionic strength between 0.1 to 0.3 M, with n < 0.43. When the ionic strength increased to 0.4 and 0.5 M, anomalous transport occurred, which is confirmed by the n values of 0.53 and 0.51, respectively. pH of the media was directly responsible for the charge of the chitosan, thereby changing the release properties, whereas, in contrast, ionic strength indirectly controls the relaxation and swelling by masking the charge. In the low Na^+ and Cl^- ion environment, chitosans' NH_3^+ groups are weakly shielded by the salt ions with a moderate swelling effect due to the electrostatic repulsion and water uptake. The release of curcumin is, therefore, dominated by the diffusion with a slight swelling effect. At higher ionic strength, Na^+ and Cl^- ions screen the NH_3^+ charges, which results in reduced swelling. However, the shielding effects allow the chitosan chains to rearrange and move freely, enhancing chain mobility. When the NaCl concentration is increased, the relaxation contribution increases in this scenario, unlike the condition for the alkaline pH where the charge of the NH_3^+ ions was neutralized. Therefore, relaxation contributes to the release of curcumin in higher ionic strength remarkably along with swelling.

When determining the drug release mechanism, the Peppas−Shalin (PS) model takes into account the contributions of both diffusion (Fickian diffusion) and polymer relaxation. The first term in the model equation (eq 10) represents the Fickian diffusional contribution (F), whereas the right side represents the Case II relaxational contribution. In all controlled-release systems, the coefficient m represents the strictly Fickian diffusion exponent. In a situation in which the bioactive substances are released only by Fickian diffusion, the PS model's m value should be equal to the KP model's n value.[95] Figure S10 displays the nonlinear curve fitting of the drug release data with the PS model equation. As described above, polymer relaxation also plays a considerable role in the release of curcumin from the biopolymer along with the Fickian diffusion. This is further confirmed by the significant differences recorded for the m values of the PS model, with the release exponent values of the KP model shown in Tables S3 and S4. The R/F ratio can be used to calculate the contribution of polymer relaxation and diffusion to the release of bioactive chemicals using the equation. According to Jadidi et al.,[96] when R/F = 1, diffusion and erosion both contribute equally to the release of the loaded drug, with diffusion predominating when R/F < 1 and relaxation (erosion) predominating when R/F > 1. Figure S15 denotes the graphical representations of the R/F against time intervals, based on the model parameters calculated using the CDR% data over 15 min time intervals. Results reveal that drug release is dominated by polymer relaxation in a majority of the media compositions with R/F > 1 after the first 15 min. Interestingly, the R/F ratio readings correspond to the values reported for the release exponent (n) in the KP model. The R/F ratios are distributed in a narrow range in the media with pH 1, 2.5 and 4, indicating the quasi-Fickian diffusion, where the diffusion also contributes to the release of the curcumin. However, a sudden increment in the R/F could be seen in the media with pH 5.5, indicating the transition phase of reaching the pK_a value (∼6.5) of chitosan, where the anomalous transports govern the release. In the media with pH 6.7, the maximal relaxation contribution can be seen compared to the diffusion (n = 0.52). Diffusion also contributes to the release of curcumin from pH 6.7 media (k_D = 0.06) as the partially protonated chitosan allows moderate swelling, with a significant chain relaxation. This relaxation contribution is reduced again in the pH range of 7.4 to 8, indicating the quasi-

Downloaded from pubs.acs.org/acsodf/article-pdf/11/28/41667/6540397/acsomega.6c01210.pdf by guest on 15 August 2026

https://doi.org/10.1021/acsomega.6c01210
ACS Omega 2026, 11, 41667−41688

Fickian diffusion with minimal relaxation due to the complete deprotonation of the polymer matrix. Similarly, the contribution of the relaxation mechanism for the curcumin release in 0.1 M−0.3 M NaCl media is of moderate value. The release behavior of the media with 0.4 and 0.5 M [NaCl] differs notably from others, as the k_D value obtained from the model fit is reported to be 0 in both scenarios. Therefore, the Fickian diffusion is not contributing to the release of the curcumin from the biopolymer, and the R/F ratio cannot be calculated. Nevertheless, the n values also confirmed the presence of elevated relaxation of the polymer matrix, by screening the + charge of the NH_3^+ group, eliminating electrostatic repulsion. The resulting chain mobility creates time-dependent release, which is similar to the coupling of diffusion and relaxation.[97] When categorized under the non-Fickian (anomalous) diffusion of the KP model, it does not distinguish the contribution of diffusion and relaxation mechanisms, but the PS model calculates these contributions. In a study conducted by Wijayawardana et al.,[44] curcumin was loaded into a chitosan polymer, and the release was studied under the same NaCl concentration range. Nonetheless, the release mechanism was dominated by quasi-Fickian diffusion (n < 0.43) even in the higher NaCl concentrations. In the current study, starch, which is a neutral polysaccharide, was incorporated into the delivery system, facilitating hydrophilicity and plasticity. Starch can enhance water uptake and disrupt the electrostatic network of chitosan, thereby improving the swelling properties and the chain mobility of the delivery system.[98] Further, starch can swell independently of the pH or ionic strength of the media,[99] creating more pores, allowing room for the relaxation of the chitosan matrix. The incorporation of starch into the delivery system has altered the release mechanism at higher NaCl concentrations, representing synergistic effects in swelling and hydrophilicity. In acidic pH levels, chitosan dominates the release *via* quasi-Fickian diffusion, while starch and chitosan act together in neutral pH for swelling and relaxation. Thus, the chitosan/starch polymeric delivery system could facilitate pH/ionic responsive drug release. Even though diffusion is responsible for the release of curcumin to a certain extent, it is not the sole governing force of the drug release from the chitosan/starch polymer matrix. The results also indicate that in some media compositions (0.4 and 0.5 M NaCl), Fickian diffusion did not contribute to the release mechanism. Relaxation was proven to contribute significantly to the release mechanism in all the tested media compositions.

The nonlinear model fits of the Higuchi model, zero-order model, first-order and Hixson−Crowell models are shown in Figures S11−S14, respectively. As Tables S3 and S4 indicate, the R^2 values recorded for the Higuchi model are relatively higher compared to the rest of the models ($R^2 \geq 0.98$). The model considers the relationship between the release rate and the square root of time, based on several assumptions. In the situation of homogeneous drug loading across the matrix, the Higuchi equation is used to describe the drug release from the nanoparticles with matrix structures, going beyond the assumption that the dissolving drug is transported only in the matrix center. The model ignores any swelling or relaxation of the polymer carrier and assumes a constant drug diffusion coefficient.[90] In most of the delivery systems, diffusion is not the only leading mechanism responsible for the release of therapeutic agents. Thus, depending solely on the data of the Higuchi model to interpret the release behaviors can lead to erroneous conclusions. It is always better to combine the findings of the Higuchi model with other delivery systems, as a single model might not capture the release behaviors of complex systems that combine multiple release mechanisms, including swelling or relaxation. That could further aid in identifying the dominant release mechanisms responsible for the release. The release constant values (k_H) of the Higuchi model align with the CDR% data and the release behavior discussed in the KP and PS models. The media, consisting of pH 1 and 7.4, exhibited a higher k_H value, where the burst effect and optimal diffusion of the curcumin were observed. When the pH values reach the pK_a value of chitosan, swelling of the polymer occurs, reaching the maximum swelling around pH 6.7. Accordingly, the lowest k_H values are recorded for these pH values (5.5 and 6.7) as the model does not consider swelling behaviors. Similarly, for the conditions with higher k_H values (pH 1 and 7.4), higher k_D (PS model) values are reported, while lower k_H values (pH 1 and 7.4) correspond to lower k_D (pH 6.7). Interestingly, the decreasing pattern of the k_H values when the [NaCl] increased correlates with the release behaviors reported for PS and KP models. Strong diffusion is demonstrated at 0.1 M NaCl with a higher k_H and k_D value (0.31 and 0.44). When the concentration of NaCl reached 0.2 and 0.3 M, the k_H and k_D values decreased, whereas the n value increased. This indicates the shift from diffusion to relaxation release behavior, where the k_H value plateaued at 0.2, showing minimal diffusion control. A significant change in these parameters can be seen when the [NaCl] drift from 0.3 to 0.4 M, when the k_H remains constant but the n drastically increases from 0.4 to 0.53, indicating a release governed by pure relaxation.

The mathematical release model developed by Hixson and Crowell (HC) describes how drug release occurs through mechanisms that show changes in particle diameter and surface area, such as a tablet in a fluid.[100] In both bioavailability assessment and medicinal applications, the Hixson-Crowell model is the most appropriate choice for accurately representing the dissolving process since it defines the drug release rate by a parameter that is completely homogeneous from batch to batch. The equation was used for specific drug dosage forms in which the drug is released in planes parallel to the drug surface.[90] The R^2 for the HC model was lower than the values reported for the above-mentioned models. Hence, the current study did not employ the HC model to understand the controlled release because it was demonstrated that the release of the curcumin was based on diffusion and relaxation rather than a continuous decrease in the polymer's surface area.

The drug dissolution of various modified-release pharmaceutical dosage forms, such as transdermal systems, matrix tablets containing poorly soluble pharmaceuticals in coated forms and osmotic systems, may be described using the zero-order model. This model, known as the ideal kinetics model, describes drugs released gradually at a constant concentration. It keeps drug levels constant in the blood plasma during delivery because the drug release rate is independent of concentration.[101] The release of an active agent under zero-order kinetics is only reliant on time, and the process proceeds at a steady pace regardless of the concentration of the active agent. The first-order model can be applied in scenarios describing drug dissolution in pharmaceutical dosage forms, such as those containing water-soluble medicines in a porous matrix. Consequently, the first-order release describes how concentration changes affect the release profiles over time. Furthermore, the first order is theoretically equal to the KP

Downloaded from pubs.acs.org/acsodf/article-pdf/11/28/41667/6540397/acsomega.6c01210.pdf by guest on 15 August 2026

https://doi.org/10.1021/acsomega.6c01210
ACS Omega 2026, 11, 41667−41688

Table 3. Summary of the Chitosan/Starch Delivery Systems Used for Curcumin

delivery system	EE%	release profile	release kinetics	targeted cell line	antibacterial activity	refs
Chitosan−starch nanocomposite for bis-des-methoxy curcumin analog	88.98%, 86.54%, and 86.60% (BDMCA-CS 3:1, 1:1 and 1:3)	Phosphate buffer (pH 7.4) BDMCA-CS 3:1—20% release (10 h), 35% release (20h), 40% (24h) BDMCA-CS 1:3—23% release (10 h), 39% reelase (20 h), 45% release (24 h)	Concentration-dependent release (First Order) polymer dissolution/erosion (Hixon-Crowell) Super case II (n value of KP model)	MCF-7 breast cancer cells and VERO cell lines	N/A	41
Carboxymethyl starch (CMS) and chitosan hydrochloride (CHC) for curcumin	89.49%−94.01%	pH 2 and pH 7.4 (SGF) Sustained release at pH 7.4	N/A	N/A	N/A	103
Starch/Chitosan Films for curcumin	81−97%	pH 1.2 20−50% release in the first hour, followed by sustained release up to 8 h.	Banana, corn, mung bean/chitosan films - diffusion-controlled process (Higuchi). Pregelatinized starch/chitosan films - Fickian diffusion	N/A	N/A	104
Chitosan/starch/MoS_2 nanocomposite for curcumin	87.25% (EE%) and 46.5% (LD%)	pHs 7.4 and 5.4 pH 5.4−96%, and for pH 7.4−79% over 96 h.	Korsmeyer-Peppas's kinetic model for an acidic environment and Higuchi's for a neutral environment, both drug releases in a non-Fick way	MCF-7	N/A	40
Chitosan/carboxymethyl starch/montmorillonite nanobiocomposite for curcumin	91%	pH 7.4, pH 4.5 pH 7.4−43% (24 h), pH 4.5 − 80% (24 h)	N/A	N/A	*Streptococcus mutans* (inhibition −95.5%, 03.7% at pH 5 and 7)	73
Starch nanoparticles for curcumin	78% (LD%)	pH 7.4 13% release-first 24 h, 93% release—240 h. Swelling-based release.	N/A	N/A	N/A	105
Lotus root amylopectin-chitosan hydrogel for curcumin	90.3%	Simulated gastric fluid (SGF) pH 2, Simulated intestinal fluid (SIF) pH 7 16%—120 min in SGF, 50% 120 min in SIF	N/A	N/A	N/A	106
Emulsion stabilized with chitosan/starch for curcumin	∼91%	*In vitro* digestion model pH 7, 5 min pH 3, 2 h. pH 7, 2 h.	80%, ∼66%, and ∼59% cumulative release for 0%, 0.1%, and 0.4% w/v CS coatings. Higuchi kinetics (KH = 32.7, 26.9, 23.4); thicker CS layers: slow diffusion.	N/A	N/A	42
Curcumin-impregnated chitosan/starch aerogels	24.1−27.6, mg per gram of aerogel (LD)	After 10 h (2 h in SGF + 8 h in SIF), released curcumin 11.1−15.9%	N/A	N/A	N/A	107
Dialdehyde starch-curcumin-gelatin-chitosan composite	N/A	75% ethanol (98.35%,48 h), water (8.91%,48 h), pH 4 (57.6%), pH 7.5 (46.6%) and pH 11 (72.0%)	PS model−non-Fickian diffusion	N/A	*E. coli* (21.4 mm) and *S. aureus* (19.9 mm), the cell survival rate treated with the film solution was 113.16%	108
Chitosan/Starch composite cross-linked with glutaraldehyde and PVA	39.7 (LD%)	pH 1−8, NaCl—0.1 M−0.5 M	Mechanisms: Fickian diffusion, relaxation, and swelling. Quasi-Fickian diffusion-acidic and alkaline pH, non-Fickian diffusion-pH 6.7. Relaxation-Higher [NaCl], diffusion and relaxation-lower [NaCl].	N/A	Enhanced antibacterial activity against *S. aureus* (15.56 ± 0.29) and *P. aeruginosa* (10.11 ± 0.44) at 20 mg/mL.	present study

https://doi.org/10.1021/acsomega.6c01210
ACS Omega 2026, 11, 41667−41688

Downloaded from pubs.acs.org/acsodf/article-pdf/11/28/41667/6540439 7/acsomega.6c01210.pdf by guest on 15 August 2026

model in cases when n = 1, indicating that the drug release is due to the case II transport mechanism.[102] For both models, relatively low R^2 values were stated, which confirms the poor fitting of the model equations to the CDR% data. Even though time and concentration can impact the release rate of the pharmaceutical formulations, that is not the responsible mechanism to describe the release pattern of curcumin from chitosan/starch composite.

In summary, a combination of Fickian diffusion, polymer relaxation and swelling controls the release of curcumin from the synthesized biopolymeric delivery system. The nonlinear curve fittings of the release data for the KP and PS models confirm the findings of the investigation. Under acidic pH conditions (pH 1−5.5), protonated chitosan NH_3^+ creates a strong electrostatic repulsion force between the polymer chains. This repulsive force, which restrains the chain mobility and the swelling, is responsible for the release mechanism dominated by quasi-Fickian diffusion (n = 0.27−0.37). Under these conditions, curcumin is released mainly through the diffusion of water-filled pores, with a lesser contribution from polymer relaxation. When the pH reaches 6.7, which is close to the pK_a value of chitosan, partial deprotonation of the chitosan occurs. This reduces the electrostatic repulsion, increasing the water uptake and thereby the chain relaxation. This behavior is reflected by the n value of the KP model (n = 0.52), suggesting that the non-Fickian diffusion, where the polymer relaxation and diffusion contribute equally to the release mechanism. The PS model further validates this phenomenon with a recorded increase in the relaxation contribution in the R/F ratio. Complete deprotonation of chitosan eliminates electrostatic repulsion in alkaline settings (pH 7.4−8), but it also decreases water absorption and polymer solubility. As a result, the release mechanism returns to quasi-Fickian diffusion (n = 0.34−0.38), where diffusion predominates over relaxation. A distinct mechanism appears at different ionic strengths. The NH_3^+ groups are weakly protected at low NaCl concentrations (0.1−0.3 M), enabling modest swelling with diffusion-controlled release (n < 0.43). Nevertheless, charge shielding by Na^+ and Cl^- ions suppress the electrostatic repulsion at higher ionic strengths (0.4−0.5 M), allowing for improved polymer chain mobility and relaxation without the swelling contribution. As demonstrated by k_D = 0 in the Peppas-Sahlin model and n values of 0.51−0.53, this leads to solely relaxation-controlled release, demonstrating anomalous transport predominantly driven by chain relaxation rather than diffusion. This behavior is further modulated by the incorporation of starch. Starch, a neutral, hydrophilic polysaccharide, improves water absorption and breaks the electrostatic network of chitosan, allowing chain relaxation. The significant relaxational contribution seen at high ionic strengths is explained by this synergistic action, which differs the composite's release behavior from that of chitosan alone.

Table 3 summarizes the data related to encapsulation efficiency, release profile, and other main biological activities of the curcumin-chitosan/starch delivery systems. However, as explained in the introduction section, these studies have not focused mainly on the aspects covered in the present study, specifically evaluating the drug release kinetics of the delivery system over a changing pH, ionic strength media, and in a concentration-dependent manner. In the current study, the antibacterial activity of the synthesized composite was also studied against 4 pathogenic bacterial species. Thus, the present work provides unique contributions for modeling the release kinetics of curcumin from chitosan/starch-based delivery systems under varying physiological conditions and evaluates a broader antibacterial profile that can be used in pharmacological applications.

Several methods for controlling the rate at which curcumin is released from the chitosan/starch composite system can be suggested for future work. Since the composite material indicated a pH-responsive release, with lower release at acidic conditions and enhanced release near pH 6.7 due to the behavior of chitosan, it is a potential targeted delivery system for the gastrointestinal environment. Ionic strength provides an additional adjustable parameter for controlling the release rate, which allows for modulation based on the ionic composition of the biological medium. Additionally, modifying the starch-to-chitosan ratio will optimize water uptake and chain relaxation contributions, while increasing the glutaraldehyde cross-linking density will tighten the polymer network and decrease release. When taken as a whole, these independent variables, including pH, ionic strength, degree of cross-linking, and chitosan: starch ratio, offer a logical foundation for synthesizing composites with customized release profiles for specific medical uses.

Chitosan used in this study was synthesized from shrimp shells and had a comparatively high molecular weight, which reduced its solubility. The swelling and release dynamics would have been different if chitosan nanoparticles had been used instead because of their larger surface area and systematic chain alignment.[109] Future research should focus on improving chitosan molecular weight and integrating nanoparticle formulations to provide a more prolonged release profile.

It is crucial to highlight that the drug release profile was plotted based on the initial release kinetics of the system to identify the governing release mechanisms under varying pH and ionic strength conditions as a necessary first step to understand the release behavior. Future studies should focus on optimizing the drug loading capacity of the delivery system and evaluating the release behavior under sink conditions, with larger volumes to obtain a complete release profile. The drug release study was designed to perform a fundamental and preliminary investigation to demonstrate the pH and ionic strength-responsive behavior of the chitosan/starch delivery system, rather than to stimulate physiological conditions. This study did not assess the potential cytotoxic effects of delivery system and its components, but these are documented as a primary limitation. Nevertheless, according to several studies, chitosan and starch nanoparticles both show better biocompatibility with low cytotoxic profiles.[110] However, a thorough safety evaluation of this particular composition *via in vivo* studies is still necessary for further biomedical applications.

4. CONCLUSIONS

Curcumin, a bioactive phytochemical with potent therapeutic effects, was loaded onto the biopolymeric delivery system consisting of chitosan and cassava starch. SEM analysis revealed that the change in surface morphology of the chitosan is due to the successful loading of starch and curcumin during the synthesis of the delivery system. FT-IR data indicated the presence of the vibrational bands of curcumin, starch, and chitosan in the composite, and the XRD pattern of the drug composite showed significant peaks corresponding to the individual components. TGA data indicated an increase in the decomposition temperature of the chitosan/starch system with the incorporation of curcumin. Similarly, BET surface area

Downloaded from pubs.acs.org/acsodf/article-pdf/11/28/41667/6540397/acsomega.6c01210.pdf by guest on 15 August 2026

https://doi.org/10.1021/acsomega.6c01210
ACS Omega 2026, 11, 41667−41688

analysis revealed the successful incorporation of starch onto the porous structure of chitosan. The antioxidant activity of the curcumin extract varied from 15.71% (0.005 mg/mL) to 81.73% (0.03 mg/mL), and the antioxidant activity of the composite varied from 10.30% (0.01 mg/mL) to 78.88% (0.06 mg/mL). Egg-albumin denaturation assay was conducted to evaluate the anti-inflammatory activity of the curcumin and composite, and the concentration range between 50 and 150 μg/mL has demonstrated better activity for the tested samples. The antibacterial studies reveal that the curcumin extract was effective against Gram-positive *S. aureus* in the tested concentration, exhibiting a dose-dependent increment in the zone of inhibition. The chitosan/starch composite displayed inhibition zones only for *P. aeruginosa*. The curcumin-coated chitosan/starch composite's antibacterial activity was effective against the growth of *P. aeruginosa* and *S. aureus*, with enhanced activity at 20 mg/mL concentration for both bacterial strains. However, neither curcumin nor curcumin-coated composite affected the growth of Gram-negative *E. coli* and *K. pneumoniae*. *A. cepa* cytotoxicity assay was used to evaluate the cytotoxic effect of the synthesized compounds, and they were tested in two concentration ranges. According to the results of the MI%, both 2.5 and 20 mg/mL concentrations were reported to exhibit no cytotoxic effect. Cumulative drug release data were fitted into kinetic models, and results indicate that both the KP and PS models had $R^2 \geq 0.99$. According to the n values of the KP model, quasi-Fickian diffusion was the predominant release mechanism of curcumin in all the pH media compositions tested except for the media with pH 6.7, where non-Fickian diffusion occurs. When the NaCl concentration increased more than 0.3, the quasi-Fickian diffusion release pattern was changed to the non-Fickian diffusion ($0.43 < n < 0.85$). PS model fit indicated that relaxation is responsible for the release of curcumin, as well as diffusion. However, in the media compositions with pH 6.7, 0.4, and 0.5 M NaCl concentration, relaxation contributes to the release predominantly, where relaxation is the only mechanism in the latter two scenarios ($k_D = 0$). These changes were attributed to the chemical composition of the media and the chitosan, where deprotonation-protonation of the NH_2 group and charge masking by the Na^+ and Cl^- regulate the swelling of the polymer matrix, resulting in the transition between quasi-Fickian and non-Fickian release mechanisms. This study consists of several limitations, including the use of higher molecular weight chitosan with limited water solubility and lack of *in vivo* experiments to evaluate the bioavailability and safety of the delivery system. A preliminary cytotoxicity assessment was carried out using the *A. cepa* root meristem model. However, this assay alone is insufficient for predicting mammalian toxicity. More rigorous evaluations using established mammalian cell lines are required to adequately characterize the biocompatibility and safety profile of the drug carrier system. Thorough *in vivo* investigations are necessary to assess the pharmacokinetics, biodistribution, and therapeutic effectiveness of this delivery method. To confirm the clinical safety and biocompatibility of the developed drug carrier, more thorough cytotoxicity evaluations and long-term toxicity studies should be conducted in future research.

■ ASSOCIATED CONTENT

Data Availability Statement

The data sets used and/or analyzed during the current study are available from the corresponding author on reasonable request.

Supporting Information

The Supporting Information is available free of charge at https://pubs.acs.org/doi/10.1021/acsomega.6c01210.

XRD pattern (Figure S1) with crystallographic parameters (Table S2); SEM images (Figure S2); TG and DTG curves (Figure S3); antibacterial mechanism illustration (Figure S4); Well diffusion results of chitosan and chitosan/starch composite against (a) *S. aureus* and (b) *P. aeruginosa*; (Figure S5); *A. cepa* root elongation test results (Figure S6); schematic illustration of the synthesis pathway and proposed interactions within the curcumin-loaded chitosan/starch/PVA composite (Figure S7); pharmacokinetic properties showing muco-adhesion, enhanced bioavailability, and systemic uptake (Figure S8); cellular lifespan of the drug composite (Figure S9); pH-dependent and ionic strength-dependent drug release kinetics data fitted with Korsmeyer-Peppas, Peppas-Sahlin, Higuchi, Zero-order, First-order, and Hixson-Crowell models (Tables S3−S4); and fitted %CDR data along with R/F values for all models under varying media conditions (Figures S10−S15) (PDF)

■ AUTHOR INFORMATION

Corresponding Author

Charitha Thambiliyagodage − *Department of Applied Sciences, Faculty of Humanities and Sciences, Sri Lanka Institute of Information Technology, Malabe 10115, Sri Lanka*; orcid.org/0000-0003-0906-4441; Email: charitha.t@sliit.lk

Authors

Lumini Abeywickrama − *Department of Applied Sciences, Faculty of Humanities and Sciences, Sri Lanka Institute of Information Technology, Malabe 10115, Sri Lanka*

Supuni Wijayawardana − *Department of Applied Sciences, Faculty of Humanities and Sciences, Sri Lanka Institute of Information Technology, Malabe 10115, Sri Lanka*

Madara Jayanetti − *Department of Applied Sciences, Faculty of Humanities and Sciences, Sri Lanka Institute of Information Technology, Malabe 10115, Sri Lanka*

Complete contact information is available at: https://pubs.acs.org/10.1021/acsomega.6c01210

Author Contributions

L.A.: Conceptualization, methodology, formal analysis, investigation, writing—original draft, visualization. S.W.: Formal analysis, investigation, writing—original draft, writing—review and editing, visualization. C.T.: Conceptualization, writing—original draft, writing—review and editing, supervision, project administration. M.J.: Methodology, supervision

Funding

Sri Lanka Institute of Information Technology funded this research project.

Downloaded from pubs.acs.org/acsodf/article-pdf/11/28/41667/6540397/acsomega.6c01210.pdf by guest on 15 August 2026

Notes

The authors declare no competing financial interest.

■ ACKNOWLEDGMENTS

The authors acknowledge the University of Moratuwa, Sri Lanka Institute of Nanotechnology, and the University of Sri Jayewardenepura for providing instrument facilities. The authors wish to thank Gevindu Masakorala, Ian Fernando, and Nethmi Jayamaha for their contribution to conducting the experiments reported in this study.

■ REFERENCES

(1) Chang, R.; Chen, L.; Qamar, M.; et al. The bioavailability, metabolism and microbial modulation of curcumin-loaded nano-delivery systems. *Adv. Colloid Interface Sci.* **2023**, *318*, No. 102933.
(2) Hegde, M.; Girisa, S.; BharathwajChetty, B.; Vishwa, R.; Kunnumakkara, A. B. Curcumin Formulations for Better Bioavailability: What We Learned from Clinical Trials Thus Far? *ACS Omega* **2023**, *8*, 10713−10746.
(3) Dehzad, M. J.; Ghalandari, H.; Nouri, M.; Askarpour, M. Antioxidant and anti-inflammatory effects of curcumin/turmeric supplementation in adults: A GRADE-assessed systematic review and dose−response meta-analysis of randomized controlled trials. *Cytokine* **2023**, *164*, No. 156144.
(4) Wang, Z.; Mu, W.; Li, P.; Liu, G.; Yang, J. Anti-inflammatory activity of ortho-trifluoromethoxy-substituted 4-piperidione-containing mono-carbonyl curcumin derivatives in vitro and in vivo. *Eur. J. Pharm. Sci.* **2021**, *160*, No. 105756.
(5) Hettiarachchi, S. S.; Perera, Y.; Dunuweera, S. P.; et al. Comparison of Antibacterial Activity of Nanocurcumin with Bulk Curcumin. *ACS Omega* **2022**, *7*, 46494−46500.
(6) Deepika; Prasad, M.; Salar, A.; Salar, R. K. In vitro anticancer activity of curcumin loaded chitosan nanoparticles (CLCNPs) against Vero cells. *Pharmacol. Res.-Mod. Chin. Med.* **2022**, *3*, No. 100116.
(7) Azzini, E.; Peña-Corona, S. I.; Hernández-Parra, H.; et al. Neuroprotective and anti-inflammatory effects of curcumin in Alzheimer's disease: Targeting neuroinflammation strategies. *Phyther. Res.* **2024**, *38*, 3169−3189.
(8) Fahmy, A. M.; Balkhi, B.; Sadek, M. A.; ElBishbishy, R. M.; Ahmed, S. PEGylated terpesomes of curcumin for prominent hepatoprotective activity: Fabrication, optimization, biochemical analysis and in vivo evaluation. *J. Drug Delivery Sci. Technol.* **2025**, *108*, No. 106876.
(9) Alduais, M. A.; El Rabey, H. A.; Mohammed, G. M.; et al. The anticancer activity of fucoidan coated selenium nanoparticles and curcumin nanoparticles against colorectal cancer lines. *Sci. Rep.* **2025**, *15*, No. 287.
(10) Ávila-Gálvez, M. Á.; González-Sarrías, A.; Martínez-Díaz, F.; et al. Disposition of Dietary Polyphenols in Breast Cancer Patients' Tumors, and Their Associated Anticancer Activity: The Particular Case of Curcumin. *Mol. Nutr. Food Res.* **2021**, *65*, No. 2100163.
(11) Bolat, Z. B.; Islek, Z.; Sahin, F.; Ucisik, M. H. Delivery of curcumin within emulsome nanoparticles enhances the anti-cancer activity in androgen-dependent prostate cancer cell. *Mol. Biol. Rep.* **2023**, *50*, 2531−2543.
(12) Wang, S.; Gao, X.; Li, J.; et al. The anticancer effects of curcumin and clinical research progress on its effects on esophageal cancer. *Front. Pharmacol.* **2022**, *13*, No. 1058070.
(13) Gao, L.; Shao, T.; Zheng, W.; Ding, J. Curcumin suppresses tumor growth of gemcitabine-resistant non-small cell lung cancer by regulating lncRNA-MEG3 and PTEN signaling. *Clin. Transl. Oncol.* **2021**, *23*, 1386−1393.
(14) Mirzaei, H.; Bagheri, H.; Ghasemi, F.; et al. Anti-Cancer Activity of Curcumin on Multiple Myeloma. *Anticancer Agents Med. Chem.* **2021**, *21*, 575−586.
(15) Zhao, J.; Jia, W.; Zhang, R.; Wang, X.; Zhang, L. Improving curcumin bioavailability: Targeted delivery of curcumin and loading systems in intestinal inflammation. *Food Res. Int.* **2024**, *196*, No. 115079.
(16) Asif, H. M.; Zafar, F.; Ahmad, K.; et al. Synthesis, characterization and evaluation of anti-arthritic and anti-inflammatory potential of curcumin loaded chitosan nanoparticles. *Sci. Rep.* **2023**, *13*, No. 10274.
(17) Liu, R.; Zhang, Y.; Deng, P.; et al. Construction of targeted delivery system for curcumin loaded on magnetic α-Fe2O3/Fe3O4 heterogeneous nanotubes and its apoptosis mechanism on MCF-7 cell. *Biomater. Adv.* **2022**, *136*, No. 212783.
(18) Zeng, Z.; Deng, S.; Liu, Y.; et al. Targeting transportation of curcumin by soybean lipophilic protein nano emulsion: Improving its bioaccessibility and regulating intestinal microorganisms in mice. *Food Hydrocolloids* **2023**, *142*, No. 108781.
(19) Ghobadi, N.; Asoodeh, A. Co-administration of curcumin with other phytochemicals improves anticancer activity by regulating multiple molecular targets. *Phyther. Res.* **2023**, *37*, 1688−1702.
(20) Saadh, M. J.; Hsu, C. Y.; Mustafa, M. A.; et al. Advances in chitosan-based blends as potential drug delivery systems: A review. *Int. J. Biol. Macromol.* **2024**, *273*, No. 132916.
(21) Liu, Z.; Wang, K.; Peng, X.; Zhang, L. Chitosan-based drug delivery systems: Current strategic design and potential application in human hard tissue repair. *Eur. Polym. J.* **2022**, *166*, No. 110979.
(22) Aslzad, S.; Heydari, P.; Abdolahinia, E. D.; et al. Chitosan/gelatin hybrid nanogel containing doxorubicin as enzyme-responsive drug delivery system for breast cancer treatment. *Colloid Polym. Sci.* **2023**, *301*, 273−281.
(23) Jalaladdiny, S. s.; Badoei-dalfard, A.; Karami, Z.; Sargazi, G. Co-delivery of doxorubicin and curcumin to breast cancer cells by a targeted delivery system based on Ni/Ta core-shell metal-organic framework coated with folic acid-activated chitosan nanoparticles. *J. Iran. Chem. Soc.* **2022**, *19*, 4287−4298.
(24) Nematollahi, E.; Pourmadadi, M.; Yazdian, F.; et al. Synthesis and characterization of chitosan/polyvinylpyrrolidone coated nanoporous γ-Alumina as a pH-sensitive carrier for controlled release of quercetin. *Int. J. Biol. Macromol.* **2021**, *183*, 600−613.
(25) Chatterjee, S.; Mahmood, S.; Hilles, A. R.; et al. Cationic starch: A functionalized polysaccharide based polymer for advancement of drug delivery and health care system - A review. *Int. J. Biol. Macromol.* **2023**, *248*, No. 125757.
(26) Lee, C. S.; Hwang, H. S. Starch-Based Hydrogels as a Drug Delivery System in Biomedical Applications. *Gels* **2023**, *9*, No. 951.
(27) Alipournazari, P.; Pourmadadi, M.; Abdouss, M.; Rahdar, A.; Pandey, S. Enhanced delivery of doxorubicin for breast cancer treatment using pH-sensitive starch/PVA/g-C3N4 hydrogel. *Int. J. Biol. Macromol.* **2024**, *265*, No. 130901.
(28) Gholamali, I.; Hosseini, S. N.; Alipour, E. Doxorubicin-loaded oxidized starch/poly (vinyl alcohol)/CuO bio-nanocomposite hydrogels as an anticancer drug carrier agent. *Int. J. Polym. Mater. Polym. Biomater.* **2021**, *70*, 967−980.
(29) Bi, W.; Liyuan, G.; Wenjuan, W.; Qiang, X. Skin targeting of resveratrol-loaded starch-based Pickering emulsions: preparation, characterization, and evaluation. *Colloid Polym. Sci.* **2021**, *299*, 1383−1395.
(30) Rajabpour, M.; Pourmadadi, M.; Yazdian, F.; Hallajisani, A.; Fazeli, A. Treatment of breast cancer with curcumin-loaded hydrogel nanocomposite containing starch/agarose/zinc oxide. *Int. J. Biol. Macromol.* **2025**, *315*, No. 144492.
(31) Parvaneh, S.; Pourmadadi, M.; Abdouss, M.; et al. Carboxymethyl cellulose/starch/reduced graphene oxide composite as a pH-sensitive nanocarrier for curcumin drug delivery. *Int. J. Biol. Macromol.* **2023**, *241*, No. 124566.
(32) Kapoor, D. U.; Pareek, A.; Sharma, M.; et al. Exploring starch-based excipients in pharmaceutical formulations: Versatile applications and future perspectives. *Eur. J. Pharm. Biopharm.* **2025**, *212*, No. 114727.
(33) Zhang, C.; Wang, X.; Xiao, M.; et al. Nano-in-micro alginate/chitosan hydrogel via electrospray technology for orally curcumin

Downloaded from pubs.acs.org/acsodf/article-pdf/11/28/41667/6540397/acsomega.6c01210.pdf by guest on 15 August 2026

https://doi.org/10.1021/acsomega.6c01210
ACS Omega 2026, 11, 41667−41688

delivery to effectively alleviate ulcerative colitis. *Mater. Des.* **2022**, *221*, No. 110894.
(34) Issarachot, O.; Bunlung, S.; Kaewkroek, K.; Wiwattanapatapee, R. Superporous hydrogels based on blends of chitosan and polyvinyl alcohol as a carrier for enhanced gastric delivery of resveratrol. *Saudi Pharm. J.* **2023**, *31*, 335−347.
(35) Liu, S.; Fang, Z.; Ng, K. Incorporating inulin and chitosan in alginate-based microspheres for targeted delivery and release of quercetin to colon. *Food Res. Int.* **2022**, *160*, No. 111749.
(36) Anand, T.; Anbukkarasi, M.; Thomas, P. A.; Geraldine, P. A comparison between plain eugenol and eugenol-loaded chitosan nanoparticles for prevention of in vitro selenite-induced cataractogenesis. *J. Drug Delivery Sci. Technol.* **2021**, *65*, No. 102696.
(37) Bahtiyar, C.; Cakir, N. T.; Kahveci, M. U.; Acik, G.; Altinkok, C. Fabrication of gallic acid containing poly(vinyl alcohol)/chitosan electrospun nanofibers with antioxidant and drug delivery properties. *Int. J. Biol. Macromol.* **2024**, *281*, No. 136055.
(38) Sarmah, D.; Rather, M. A.; Sarkar, A.; et al. Self-cross-linked starch/chitosan hydrogel as a biocompatible vehicle for controlled release of drug. *Int. J. Biol. Macromol.* **2023**, *237*, No. 124206.
(39) Nguyen, V. N.; Wang, S. L.; Nguyen, T. H.; et al. Preparation and Characterization of Chitosan/Starch Nanocomposites Loaded with Ampicillin to Enhance Antibacterial Activity against *Escherichia coli*. *Polymers* **2024**, *16*, No. 2647.
(40) Omrani, Z.; Pourmadadi, M.; Yazdian, F.; Rashedi, H. Preparation and characterization of pH-sensitive chitosan/starch/MoS2 nanocomposite for control release of curcumin macromolecules drug delivery; application in the breast cancer treatment. *Int. J. Biol. Macromol.* **2023**, *250*, No. 125897.
(41) Subramanian, S. B.; Francis, A. P.; Devasena, T. Chitosan−starch nanocomposite particles as a drug carrier for the delivery of bisdesmethoxy curcumin analog. *Carbohydr. Polym.* **2014**, *114*, 170−178.
(42) Jo, M.; Ban, C.; Goh, K. K. T.; Choi, Y. J. Enhancement of the intestinal permeability of curcumin using Pickering emulsions stabilized by starch crystals and chitosan. *Food Chem.* **2023**, *405*, No. 134889.
(43) Mendis, A.; Thambiliyagodage, C.; Ekanayake, G.; et al. Fabrication of Naturally Derived Chitosan and Ilmenite Sand-Based TiO2/Fe2O3/Fe-N-Doped Graphitic Carbon Composite for Photocatalytic Degradation of Methylene Blue under Sunlight. *Molecules* **2023**, *28*, No. 3154, DOI: 10.3390/molecules28073154.
(44) Wijayawardana, S.; Thambiliyagodage, C.; Jayanetti, M. Kinetic study of in vitro release of curcumin from chitosan biopolymer and the evaluation of biological efficacy. *Arab. J. Chem.* **2024**, *17*, No. 105896.
(45) Karua, C. S.; Sahoo, A. Synthesis and characterization of starch/chitosan composites. *Mater. Today: Proc.* **2020**, *33*, 5179−5183.
(46) Jayanetti, M.; Thambiliyagodage, C.; Liyanaarachchi, H. In vitro influence of PEG functionalized ZnO − CuO nanocomposites on bacterial growth. *Sci. Rep.* **2024**, *14*, No. 1293.
(47) Wijeyaratne, W. M. D. N.; Wadasinghe, L. G. Y. J. G. Allium cepa Bio Assay to Assess the Water and Sediment Cytogenotoxicity in a Tropical Stream Subjected to Multiple Point and Nonpoint Source Pollutants. *J. Toxicol.* **2019**, *2019*, No. 5420124.
(48) Torres-Bugarín, O.; Gómez-Ferreyra, I.; Contreras-Dueñas, M.; et al. The Allium cepa Assay as a Versatile Tool for Genotoxicity and Cytotoxicity: Methods, Applications, and Comparative Insight. *Appl. Biosci.* **2026**, *5*, No. 9.
(49) Rukshan, R.; Rajapaksha, N.; Wijayawardana, S.; et al. Fe3O4−Chitosan Nanocomposite as a pH-Responsive Delivery System for Enhanced Delivery of Punica Granatum L. Polyphenols. *ACS Omega* **2025**, *10*, 50488−50510.
(50) Khatun, M.; Nur, M. A.; Biswas, S.; Khan, M.; Amin, M. Z. Assessment of the anti-oxidant, anti-inflammatory and anti-bacterial activities of different types of turmeric (Curcuma longa) powder in Bangladesh. *J. Agric. Food Res.* **2021**, *6*, No. 100201, DOI: 10.1016/j.jafr.2021.100201.
(51) Tanvir, E. M.; Hossen, M. S.; Hossain, M. F.; et al. Antioxidant Properties of Popular Turmeric (Curcuma longa) Varieties from Bangladesh. *J. Food Qual.* **2017**, *2017*, No. 8471785.
(52) Ciochina, R.; Savella, C.; Cote, B.; Chang, D.; Rao, D. Synthesis and characterization of new curcumin derivatives as potential chemotherapeutic and antioxidant agents. *Drug Dev. Res.* **2014**, *75*, 88−96.
(53) Yu, F.; Luo, H.; Wang, Y.; et al. Preparation of curcumin-loaded chitosan/lecithin nanoparticles with increased anti-oxidant activity and in vivo bioavailability. *Int. J. Biol. Macromol.* **2024**, *281*, No. 136659.
(54) Liu, Q.; Xie, M.; Li, X.; et al. Development of curcumin-loaded hyaluronic acid complexes for curcumin intestinal delivery: Preparation, characterization, antioxidant, and in vitro digestive properties. *LWT* **2024**, *214*, No. 117164.
(55) O'Toole, M. G.; Soucy, P. A.; Chauhan, R.; et al. Release-Modulated Antioxidant Activity of a Composite Curcumin-Chitosan Polymer. *Biomacromolecules* **2016**, *17*, 1253−1260.
(56) Tomida, H.; Fujii, T.; Furutani, N.; et al. Antioxidant properties of some different molecular weight chitosans. *Carbohydr. Res.* **2009**, *344*, 1690−1696.
(57) Hromis, N.; Lazic, V.; Popovic, S.; Suput, D.; Bulut, S. Antioxidative activity of chitosan and chitosan based biopolymer film. *Food Feed Res.* **2017**, *44*, 91−100.
(58) Alsharabasy, A. Semi-synthesis of Chitosan with High Molecular Weight and Enhanced Deacetylation Degree Amir. *Polym. Sci.* **2016**, *2*, 1−8.
(59) Belma, P.; Kenan, Č.; Dina, L.; et al. Curcumin: Natural Antimicrobial and Anti Inflammatory Agent. *J. Pharm. Res. Int.* **2021**, *32*, 1−8.
(60) Rinkunaite, I.; Simoliunas, E.; Alksne, M.; Dapkute, D.; Bukelskiene, V. Anti-inflammatory effect of different curcumin preparations on adjuvant-induced arthritis in rats. *BMC Complementary Med. Ther.* **2021**, *21*, No. 39.
(61) Xue, H.; Feng, J.; Tang, Y.; et al. Research progress on the interaction of the polyphenol−protein−polysaccharide ternary systems. *Chem. Biol. Technol. Agric.* **2024**, *11* (11), No. 95.
(62) Trigo-gutierrez, J. K.; Vega-chacón, Y.; Soares, A. B.; de Oliveira Mima, E. G. Antimicrobial activity of curcumin in nanoformulations: A comprehensive review. *Int. J. Mol. Sci.* **2021**, *22*, No. 7130.
(63) Atay, H. Y.Antibacterial Activity of Chitosan-Based Systems. In *Functional Chitosan Drug Delivery in Biomedical Applications*; Springer, 2019; pp 457−489 .
(64) Shehabeldine, A.; Hasanin, M. Green synthesis of hydrolyzed starch−chitosan nano-composite as drug delivery system to gram negative bacteria. *Environ. Nanotechnology, Monit. Manage.* **2019**, *12*, No. 100252.
(65) Sakeer, K.; Ispas-Szabo, P.; Benyerbah, N.; Mateescu, M. A. Ampholytic starch excipients for high loaded drug formulations: Mechanistic insights. *Int. J. Pharm.* **2018**, *535*, 201−216.
(66) Hosseinnejad, M.; Jafari, S. M. Evaluation of different factors affecting antimicrobial properties of chitosan. *Int. J. Biol. Macromol.* **2016**, *85*, 467−475.
(67) Ardean, C.; Davidescu, C. M.; Nemeş, N. S.; et al. Factors influencing the antibacterial activity of chitosan and chitosan modified by functionalization. *Int. J. Mol. Sci.* **2021**, *22*, No. 7449.
(68) Huszczynski, S. M.; Lam, J. S.; Khursigara, C. M. The role of Pseudomonas aeruginosa lipopolysaccharide in bacterial pathogenesis and physiology. *Pathogens* **2020**, *9*, No. 6, DOI: 10.3390/pathogens9010006.
(69) Adamczak, A.; Ożarowski, M.; Karpiński, T. M. Curcumin, a Natural Antimicrobial Agent with.pdf. *Pharmaceuticals* **2020**, *13*, No. 153.
(70) Górski, M.; Niedźwiadek, J.; Magryś, A. Antibacterial activity of curcumin − a natural phenylpropanoid dimer from the rhizomes of Curcuma longa L. and its synergy with antibiotics. *Ann. Agric. Environ. Med.* **2022**, *29*, 394−400.

Downloaded from pubs.acs.org/acsodf/article-pdf/11/28/41667/6540397/acsomega.6c01210.pdf by guest on 15 August 2026

(71) Dai, C.; Lin, J.; Li, H.; et al. The Natural Product Curcumin as an Antibacterial Agent: Current Achievements and Problems. *Antioxidants* **2022**, *11*, No. 459, DOI: 10.3390/antiox11030459.
(72) Li, Y.; Wang, Y.; Zhao, J.; Li, Z.; Chen, H. International Journal of Biological Macromolecules A pH-sensitive curcumin loaded microemulsion- fi lled alginate and porous starch composite gels: Characterization, in vitro release kinetics and biological activity. *Int. J. Biol. Macromol.* **2021**, *182*, 1863−1873.
(73) Jahanizadeh, S.; Yazdian, F.; Marjani, A.; Omidi, M.; Rashedi, H. Curcumin-loaded chitosan/carboxymethyl starch/montmorillonite bio-nanocomposite for reduction of dental bacterial biofilm formation. *Int. J. Biol. Macromol.* **2017**, *105*, 757−763.
(74) Zeinab, B.; Buthaina, J.; Rafik, K. Resistance of Gram-Negative Bacteria to Current Antibacterial Agents and Approaches to Resolve It. *Molecules* **2023**, *25*, No. 1340.
(75) Shariatinia, Z.; Fazli, M. Mechanical properties and antibacterial activities of novel nanobiocomposite films of chitosan and starch. *Food Hydrocolloids* **2015**, *46*, 112−124.
(76) Itzia Azucena, R.-C.; José Roberto, C. L.; Martin, Z. R.; et al. Drug Susceptibility Testing and Synergistic Antibacterial Activity of Curcumin with Antibiotics against Enterotoxigenic *Escherichia coli*. *Antibiotics* **2019**, *8*, No. 43.
(77) Yadav, S.; Singh, A. K.; Agrahari, A. K.; et al. Galactose-clicked curcumin-mediated reversal of Meropenem resistance among klebsiella pneumoniae by targeting its carbapenemases and the AcrAB-TolC efflux system. *Antibiotics* **2021**, *10*, No. 388, DOI: 10.3390/antibiotics10040388.
(78) Antosiewicz, D. Analysis of the cell cycle in the root meristem of Allium cepa under the influence of ledakrin - PubMed. *Folia Histochem. Cytobiol.* **1990**, *26*, 79−95.
(79) Yamamura, R.; Inoue, K. Y.; Nishino, K.; Yamasaki, S. Intestinal and fecal pH in human health. *Front. Microbiomes* **2023**, *2*, No. 1192316.
(80) Leslie, T. K.; James, A. D.; Zaccagna, F.; et al. Sodium homeostasis in the tumour microenvironment. *Biochim. Biophys. Acta Rev. Cancer* **2019**, *1872*, No. 188304.
(81) Regnery, S.; Behl, N. G.; Platt, T.; et al. Ultra-high-field sodium MRI as biomarker for tumor extent, grade and IDH mutation status in glioma patients. *NeuroImage Clin.* **2020**, *28*, No. 102427.
(82) James, A. D.; Leslie, T. K.; Kaggie, J. D.; et al. Sodium accumulation in breast cancer predicts malignancy and treatment response. *Br. J. Cancer* **2022**, *127*, 337−349.
(83) Barrett, T.; Riemer, F.; McLean, M. A.; et al. Quantification of Total and Intracellular Sodium Concentration in Primary Prostate Cancer and Adjacent Normal Prostate Tissue with Magnetic Resonance Imaging. *Invest. Radiol.* **2018**, *53*, 450−456.
(84) Jafari, M.; Parastouei, K.; Abbaszadeh, S. Development of curcumin-loaded nanoemulsion stabilized with texturized whey protein concentrate: Characterization, stability and in vitro digestibility. *Food Sci. Nutr.* **2024**, *12*, 1655−1672.
(85) Ostovar, S.; Pourmadadi, M.; Shamsabadipour, A.; Mashayekh, P. Nanocomposite of chitosan/gelatin/carbon quantum dots as a biocompatible and efficient nanocarrier for improving the Curcumin delivery restrictions to treat brain cancer. *Int. J. Biol. Macromol.* **2023**, *242*, No. 124986.
(86) Rajabzadeh-Khosroshahi, M.; Pourmadadi, M.; Yazdian, F.; et al. Chitosan/agarose/graphitic carbon nitride nanocomposite as an efficient pH-sensitive drug delivery system for anticancer curcumin releasing. *J. Drug Delivery Sci. Technol.* **2022**, *74*, No. 103443.
(87) Feyissa, Z.; Edossa, G. D.; Bedasa, T. B.; Inki, L. G. Fabrication of pH-Responsive Chitosan/Polyvinylpyrrolidone Hydrogels for Controlled Release of Metronidazole and Antibacterial Properties. *Int. J. Polym. Sci.* **2023**, *2023*, No. 1205092.
(88) Tamer, T. M.; Abbas, R.; Sadik, W. A.; et al. Development of novel amino-ethyl chitosan hydrogel for the removal of methyl orange azo dye model. *Sci. Rep.* **2024**, *14*, No. 1284.
(89) Algharib, S. A.; Dawood, A.; Zhou, K.; et al. Preparation of chitosan nanoparticles by ionotropic gelation technique: Effects of formulation parameters and in vitro characterization. *J. Mol. Struct.* **2022**, *1252*, No. 132129.
(90) Askarizadeh, M.; Esfandiari, N.; Honarvar, B.; Sajadian, S. A.; Azdarpour, A. Kinetic Modeling to Explain the Release of Medicine from Drug Delivery Systems. *ChemBioEng Rev.* **2023**, *10*, 1006−1049.
(91) Viswanadha, L. S.; Arcot, Y.; Lin, Y. T.; Akbulut, M. E. S. A comparative investigation of release kinetics of paclitaxel from natural protein and macromolecular nanocarriers in nanoscale drug delivery systems. *JCIS Open* **2024**, *15*, No. 100120.
(92) Bayer, I. S. Controlled Drug Release from Nanoengineered Polysaccharides. *Pharmaceutics* **2023**, *15* (15), No. 1364.
(93) Yadav, M.; Kaushik, B.; Rao, G. K.; Srivastava, C. M.; Vaya, D. Advances and challenges in the use of chitosan and its derivatives in biomedical fields: A review. *Carbohydr. Polym. Technol. Appl.* **2023**, *5*, No. 100323.
(94) Naderi, Z.; Azizian, J. Synthesis and characterization of carboxymethyl chitosan/Fe3O4 and MnFe2O4 nanocomposites hydrogels for loading and release of curcumin. *J. Photochem. Photobiol. B: Biol.* **2018**, *185*, 206−214.
(95) Unagolla, J. M.; Jayasuriya, A. C. Drug transport mechanisms and in vitro release kinetics of vancomycin encapsulated chitosan-alginate polyelectrolyte microparticles as a controlled drug delivery system. *Eur. J. Pharm. Sci.* **2018**, *114*, 199−209.
(96) Jadidi, A.; Davoodian, F.; Salahinejad, E. Effect of poly lactic-co-glycolic acid encapsulation on drug delivery kinetics from vancomycin-impregnated Ca-Mg silicate scaffolds. *Prog. Org. Coat.* **2020**, *149*, No. 105970, DOI: 10.1016/j.porgcoat.2020.105970.
(97) Brazel, C. S.; Peppas, N. A. Modeling of drug release from Swellable polymers. *Eur. J. Pharm. Biopharm.* **2000**, *49*, 47−58.
(98) Boldrini, D. E. Starch-based materials for drug delivery in the gastrointestinal tract-A review. *Carbohydr. Polym.* **2023**, *320*, No. 121258.
(99) Lee, C. H.; Chin, K. B. Influence of the pH and Salt Concentrations on Physicochemical Properties of Pork Myofibrillar Protein Gels Added with Cornstarch. *Food Sci. Anim. Resour.* **2020**, *40*, 254−261.
(100) Molavi, F.; Hamishehkar, H.; Nokhodchi, A. Impact of Tablet Shape on Drug Dissolution Rate Through Immediate Released Tablets. *Adv. Pharm. Bull.* **2020**, *10*, 656−661.
(101) Ahmed, L.; Atif, R.; Eldeen, T. S.; et al. Study the Using of Nanoparticles as Drug Delivery System Based on Mathematical Models for Controlled Release. *Int. J. Latest Technol. Eng. Manage. Appl. Sci.* **2019**, *8*, 52−56.
(102) Jiang, K.; Zhou, X.; He, T. The synthesis of bacterial cellulose-chitosan zwitterionic hydrogels with pH responsiveness for drug release mechanism of the naproxen. *Int. J. Biol. Macromol.* **2022**, *209*, 814−824.
(103) Li, X. M.; Wu, Z. Z.; Zhang, B.; et al. Fabrication of chitosan hydrochloride and carboxymethyl starch complex nanogels as potential delivery vehicles for curcumin. *Food Chem.* **2019**, *293*, 197−203.
(104) Siripruekpong, W.; Issarachot, O.; Kaewkroek, K.; Wiwattanapatapee, R. Development of Gastroretentive Carriers for Curcumin-Loaded Solid Dispersion Based on Expandable Starch/Chitosan Films. *Moecules* **2023**, *28*, No. 361.
(105) Chin, S. F.; Mohd Yazid, S. N. A.; Pang, S. C. Preparation and characterization of starch nanoparticles for controlled release of curcumin. *Int. J. Polym. Sci.* **2014**, *2014*, 2−9, DOI: 10.1155/2014/340121.
(106) Liu, K.; Huang, R. L.; Zha, X. Q.; et al. Encapsulation and sustained release of curcumin by a composite hydrogel of lotus root amylopectin and chitosan. *Carbohydr. Polym.* **2020**, *232*, No. 115810.
(107) Alavi, F.; Ciftci, O. N. Green and single-step simultaneous composite starch aerogel formation-high bioavailability curcumin particle formation. *Int. J. Biol. Macromol.* **2024**, *264*, No. 129945.
(108) Li, H.; Jiang, Y.; Yang, J.; et al. Preparation of curcumin-chitosan composite film with high antioxidant and antibacterial capacity: Improving the solubility of curcumin by encapsulation of biopolymers. *Food Hydrocolloids* **2023**, *145*, No. 109150.

Downloaded from pubs.acs.org/acsodf/article-pdf/11/28/41667/6540397/acsomega.6c01210.pdf by guest on 15 August 2026

(109) Yari, K.; Gharati, G.; Akbari, I. Evaluating effect of salt leaching method on release and swelling rate of metformin nanoparticles loaded-chitosan/polyvinyl alcohol porous composite. *Int. J. Biol. Macromol.* **2023**, *227*, 1282−1292.
(110) Lian, R.; Cao, J.; Jiang, X.; Rogachev, A. V. Physicochemical, antibacterial properties and cytocompatibility of starch/chitosan films incorporated with zinc oxide nanoparticles. *Mater. Today Commun.* **2021**, *27*, No. 102265.

Downloaded from pubs.acs.org/acsodf/article-pdf/11/28/41667/6540397/acsomega.6c01210.pdf by guest on 15 August 2026

https://doi.org/10.1021/acsomega.6c01210
ACS Omega 2026, 11, 41667−41688